

## **Chromite and PGE in the Logar Ophiolite Complex, Afghanistan**

A. J. Benham<sup>1</sup>, P. Kováč<sup>2</sup>, M. G. Petterson<sup>1</sup>, I. Rojkovic<sup>3</sup>, M. T. Styles<sup>1</sup>, A. G. Gunn<sup>1</sup>,  
J. A. McKervey<sup>1</sup>, A. Wasy<sup>4</sup>

<sup>1</sup>British Geological Survey, Keyworth, Nottingham NG 12 5GG, UK, e-mail:

[abenham@bgs.ac.uk](mailto:abenham@bgs.ac.uk)

<sup>2</sup>GET Limited, Partizanska cesta 3, 974 01 Banska Bystrica, Slovakia

<sup>3</sup> Geological Institute Slovak Academy of Sciences, Dúbravska cesta 9, 840 06  
Bratislava, Slovakia

<sup>4</sup> Afghanistan Geological Survey, Kabul, Afghanistan

- the number of words of text – 5 264
- the number of references – 52
- the number of tables and figures – figures 21 tables 3

- an abbreviated title (< 40 characters)

Chromite and PGE from Logar, Afghanistan

## **Abstract**

The Logar Ophiolite Complex (LOC) is located 30 km south of Kabul, Afghanistan, and extends over approximately 2000 km<sup>2</sup>. It comprises a lower lherzolitic-dunitic-harzburgitic-gabbro ultramafic-mafic unit that passes upwards into a dolerite dyke complex, basaltic pillow lavas and an uppermost sequence of volcanoclastic- and terrigenous-dominated sedimentary units. The ophiolite represents an obducted remnant of intra-Tethyan basin oceanic crust, thrust onto a platform-style cover component of the Kabul Terrane during the Himalayan orogeny.

Platinum-group minerals have been detected for the first time in chromitites and ultramafic units from the LOC. Two distinct types of chromitites and ultramafic lithologies with different origins have also been identified in this study. The first type is a low Cr, PGE-poor chromitite interpreted to have been produced in a mid ocean ridge (MOR) environment. The second type is a high Cr, relatively PGE-rich dunite and peridotite from a boninitic magma produced in a supra-subduction zone (SSZ) setting. Platinum group element (PGE) abundances in these chromitites average 12 ppb and 26 ppb for Pt+Pd+Rh for the dunite and peridotite.

Chondrite-normalised PGE patterns have two distinct trends: (1) The MOR rocks have a positive Ru anomaly with a negative Pt anomaly and a generally negative slope; and (2) the SSZ rocks show weak positive Ru and Pt anomalies and a positive slope. It is concluded that the negative sloping pattern is typical of PGE in most ophiolites elsewhere. In contrast, the positively sloping pattern is more unusual and may indicate PGE remobilisation and enrichment.

## **Introduction**

The Logar Ophiolite Complex (LOC) is located about 30 km south of Kabul, Afghanistan (Figure 1). The ophiolite has an approximately ellipsoidal outcrop, elongated in a north-north-westerly direction. It covers an area of approximately 2000 km<sup>2</sup> and is about 65 km long by 45 km wide<sup>43</sup>. Chromite mineralisation has been known from Logar Province for many years<sup>48, 41, 42</sup> but previous scientific investigations have mostly focussed on the formation and structure of the LOC<sup>29, 43</sup>. This paper presents the first modern research into chromite and platinum-group elements (PGE) in Afghanistan since the withdrawal of Soviet troops in 1989.

## **Review of geological research**

### **Geological setting of the Logar area**

Afghanistan has a long and complicated tectonic history, partly related to its position at the western end of the Himalaya mountain range. The country is composed of a series of discrete tectonic crustal blocks separated by fault zones. The blocks accreted during a series of tectonic events related to the closure of the Tethys Ocean and the collision of Laurasia with Gondwanaland in Jurassic to early Cretaceous times. A simplified tectonic map of Afghanistan illustrating the different terranes is shown in Figure 2.

There are several major tectonic units in the Logar area: the basement of the Central Afghanistan Terrane, the platform-type cover sequence of the Kabul Terrane and the Logar Ophiolite Complex. The basement of the Central Afghanistan Terrane (the Central Afghanistan Median Block according to previous studies<sup>18, 13, 30</sup>) is composed of the Early to Mid Proterozoic Sherdarwaza Formation, consisting of gneisses and schists regionally metamorphosed to amphibolite facies, and the Late Proterozoic Welayati Formation. The lower part of the Welayati Formation consists mainly of amphibolites whilst the upper part comprises schists and amphibolites with layers of plagiogranites, quartzites and marbles. The total thickness of these units is believed to be 4 800 to 5 500 m<sup>18, 13</sup>.

The platform-type cover sequence of the Kabul Terrane unconformably overlies the Central Afghanistan Terrane and is represented by the Late Permian to Mid Jurassic Chingil Formation. The Late Permian Chingil Formation comprises a basal sequence of quartz-mica schists, quartz sandstones and conglomerate overlain by approximately 350 m of calcite marbles, coralline-crinoidal-, brachiopod- and fusulinid-bearing dolomite marbles. The Late Permian rocks pass gradationally into 40 - 50 m of Early Triassic lithologies comprising yellow-pinkish dolomite and calcite marbles, and dark-brown variegated shaley limestones. These are conformably overlain by 400 – 500 m thick package of Mid Triassic dark-grey thickly bedded dolomite marbles. The Mid Triassic units pass upwards into a 70 m thick sequence of Late Triassic dark-grey, thickly-bedded calcite marbles, with thin intercalations of schists with gastropod- and pelecypod-rich, sandy limestones. Early Jurassic rocks of the Chingil Formation (200 – 250 m thick) comprise dolomite and limestone marbles, calcareous schists with rare intercalations of sandy, oolitic limestones. Mid Jurassic rocks consist of pale and dark coloured limestone marbles, with rare intercalations of carbonate schists, about 100 – 150 m thick.

The Neogene Latabang Formation (400 - 500 m) overlies rocks of the Chingil Formation. It is composed of clay, marl, sandstone and conglomerate. It contains remnants of gastropods, plants and fish skeletons, which prove its Neogene age.

The LOC represents an obducted remnant of oceanic crust that was thrust over the Kabul Terrane during the Himalayan orogeny. The ophiolite is bounded to the west by the steeply dipping (60-70°), roughly north-south-trending, Pagman Fault, while the Altimur Fault occurs to the east and south-east. The Abparan Thrust separates the allochthonous ultramafic rocks from the autochthonous rocks of the Kabul Block to the north (Figure 3).

### **The Logar Ophiolite Complex**

The German geologist Wirtz first described the LOC in 1964<sup>49</sup>. Between 1964-1966 1:100 000 and 1:50 000 geological mapping of the Kabul Block, including the LOC, was undertaken by the Department of Geology and Mines Survey of Afghanistan<sup>5</sup>. Since 1969 all geological mapping has been carried out by the Survey with technical

assistance from the USSR. Soviet and Afghan geologists undertook a series of surveys throughout Afghanistan in the 1970s, including mineral exploration in the Kabul district, which includes the Logar area<sup>15</sup>.

The Federal Institute for Soil Research, the precursor to the German Geological Survey, undertook further surface mapping of the ultramafic rocks in the Logar area, together with detailed chemical and mineralogical scientific studies<sup>42</sup>. Hafisi<sup>21</sup> also carried out PhD research on the LOC providing additional geological, mineralogical and petrographic information on the ultramafic rock units of the ophiolite, but he appears not to have studied the chromite mineralisation.

The LOC is composed of several discrete litho-stratigraphical structural units and associated volcano-sedimentary units. The lowest stratigraphic part of the LOC consists of the Ultramafic Complex, which is overlain by a thin gabbro unit and then a dyke complex and a pillow lava complex (Figure 4). This is overlain by the volcano-sedimentary sequence of the Petau Formation, which is in turn overlain by the Mana Formation, representing a sequence of accretionary wedge sediments.

The Ultramafic Complex<sup>48, 5, 45, 13, 29, 30, 1</sup> is believed to be Early Cretaceous in age since the lower, shallow water, volcano-sedimentary part of the underlying Petau Formation is dated Early Cretaceous and the upper part of the Petau Formation is Late Cretaceous<sup>30</sup>.

The main part of the Ultramafic Complex comprises largely dunite and harzburgite, with minor lherzolite, wehrlite, serpentinite and serpentinite breccia (Figure 4). The upper part of the complex comprises layered ultramafic to mafic rocks of which the uppermost part consists of melanocratic layered gabbro. The Ultramafic Complex is up to 2 800 m thick and hosts sporadic podiform chromite mineralization. A typical view of the Ultramafic Complex is seen in Figure 5.

The central part of the Ultramafic Complex sequence contains a dolerite dyke complex. Most of the dykes strike north-east and are steeply dipping (approximately 70 - 80°), or sub vertical. The thickness of the dykes varies from 1 - 15 m and they can be traced along strike up to 5 km. The dykes comprise dolerite, with minor

andesite-basalt, dolerite and gabbro-diorite or microgabbro. The age of the dyke complex is considered to be Early Cretaceous<sup>30</sup>.

The pillow lava complex, (Figure 4), comprises dark grey–green aphyric or porphyritic spilite to basaltic or andesitic pillow lavas with rare layers of volcanic breccia, tuff, agglomerate tuff and breccia tuff. It is up to 1 700-1 800 m thick. There are also occasional layers and lenses of radiolarite, hyaloclastite and dark muddy limestone. The age obtained by U-Pb dating from the andesitic basalt is 86 Ma<sup>30</sup>, which corresponds to the Late Cretaceous. The pillow lava complex was formed in a deep ocean-floor environment and overlays layered gabbro-norite rocks of the upper part of the Ultramafic Complex.

## **Chromite mineralisation in the LOC**

### **Previous work**

The United States Bureau of Mines (USBM) first recognised chromite mineralisation in the Logar area in 1949-50<sup>48</sup>. This work identified ten outcropping chromite deposits, numbered 1 to 10, occurring as massive lenses, pods and irregular-shaped bodies of dominantly massive chromitite. Subsequent work by the Federal Institute for Soil Research<sup>41, 42</sup>, recognised 18 lenticular chromite bodies including some previously identified by USBM.

The chromite bodies occur in two principal groups approximately 9 km apart, with most occurring on the west side of the Logar valley. All deposits are easily accessible from the tarred Kabul-Gardez road running alongside the Logar River (Figure 6). A northern cluster of deposits is located approximately 7 km north-west of the village of Muhammad Agha, while a southern cluster occurs to the south-west of Dewalak, about 5 km south of Muhammad Agha. The chromite bodies occur predominantly within small dunite pods in harzburgite according to Siebrat<sup>42</sup>. Kilometre-sized bodies of lherzolite and later cross-cutting orthopyroxenite dykes are also commonly associated with outcrops of chromite. Although Hafisi<sup>21</sup> mapped much of the country rock of the northern chromite belt as dunite, new work from this study has identified harzburgite as well as dunite associated with chromite occurrences, which agrees with Siebrat's original interpretation<sup>42</sup>. The observed association of rock types suggest

this is the upper part of the mantle sequence close to the mantle transition zone (MTZ)<sup>23</sup>.

Little is reported to remain at surface for most of these deposits as most of the chromite has been quarried<sup>42</sup>. In general, the deposits are reported to have been relatively small with dips between 32-45° towards the south-west. However, the largest deposit, termed number 5 by the USBM<sup>48</sup>, comprised two lenses, one 97.5 m long and up to 10 m wide, and the other 65 m long and up to 5 m wide. The margins of all the chromite bodies are sharp and highly irregular in form, whilst the immediate wallrocks are generally serpentinitised and showed the development of a close-spaced planar fabric / fracturing parallel to the contact with the chromitite.

The USBM also undertook trenching, sampling by shallow percussion drilling, and a diamond-drilling programme in which 27 holes were drilled with an aggregate length of 975 m<sup>48</sup>. The diamond drilling tested three of the largest deposits at surface and also a small high-grade deposit, all situated in the northern cluster of deposits. Volin<sup>48</sup> estimated a total 'reserve' of 181 000 t, concentrated in three deposits (1, 2 and 5). Of this about 15% (27 000 t) is high-grade metallurgical chromite with 55.9% Cr<sub>2</sub>O<sub>3</sub> and a Cr:Fe ratio of 3.5:1. The remainder of the 'reserve' contains less than 45% Cr<sub>2</sub>O<sub>3</sub> and high levels of Al<sub>2</sub>O<sub>3</sub>. The majority (92%) of the total 'reserve' occurs in the three largest deposits (numbers 2, 5 and 7), and of these, only deposit 2 contains high-grade ore. Subsequent work by Siebdrat<sup>41,42</sup> increased the USBM's chromite resource estimates to approximately 3 000 000 t "visible or probable", and a further 200 000 t "possible". It is unclear whether these figures conform to any mineral resource reporting system of the time, or whether this was based on additional drilling or new geophysical data.

Soviet and Afghan geologists undertook a 1:500 000 scale geological mapping programme in the Kabul district during the 1970s. An initial survey identified copper, chromite, beryl, mica, graphite and asbestos occurrences in this area<sup>15</sup>. A later survey identified additional chromite bodies in the Logar ophiolite, though these were commonly isolated lenses a few metres in size and were not considered to be economic<sup>30</sup>. No modern geological mapping or mineral resource assessment has been undertaken in the area since the withdrawal of Soviet troops in 1989.

## **New work**

Two disused chromite quarries were visited in November 2006. Security considerations precluded the study of other localities within the LOC. The first locality, hereafter referred to as C1, (34° 13' 16.4" N, 69° 2' 29.1" E), is a disused quarry approximately 20 m long by 10 m wide and with a maximum depth of 20 m from surface (Figure 7). Nine samples, mostly of chromite or pyroxenite, were collected in or around C1. The mineralisation remaining in place consists of massive chromite in the footwall of the northern end of the quarry (Figure 8), areas of disseminated mineralisation with occasional blebs of chromite associated with 1-2 cm thick carbonate veins (Figure 9), and occasional sub-massive chromite mineralisation (Figure 10). Although the visible chromite pods are small, generally a few metres in length by up to a metre in width, there were indications that larger chromite bodies had been previously worked. Mineralisation in the side of the quarry indicated that one of these bodies, most of which was now worked out, was approximately 50 m long and 8 m wide and dipped at 49°W. A narrow, discordant, possibly lenticular, body of pyroxenite/wehrlite up to 200-300 m long and about 1m thick is exposed on the western edge of the quarry oriented at 146° (Figure 11).

The second locality visited, hereafter referred to as C2, (34° 13' 43.6" N, 69° 1' 34.3" E), was another disused chromite quarry approximately 60 m long by 30 m wide and up to 20 m deep (Figure 12). The quarry exploited podiform chromite cropping out in the side of a hill but little mineralisation remains in situ. Several small massive chromite lenses are seen in the quarry walls associated with extensive carbonate veining and serpentinitisation. A narrow, dyke-like body of pyroxenite/wehrlite, up to 1 m thick, was traced uphill from the quarry for approximately 200 m. Additional minor chromite lenses (1-2 m in length and 30 cm in width) were also observed further up slope from the quarry. Most chromitite outcrops have been previously excavated, at least in part, in order to determine their shape and size. Five samples of chromitite and pyroxenite were taken in and around C2.

## **Petrological and mineralogical studies**

## **Methodology**

Polished thin sections from 12 rock samples collected at C1 and C2 were examined using petrological microscopes at the British Geological Survey (BGS), UK. These samples comprised five chromitites, three dunites, two pyroxenites, one peridotite and one sample of microgabbro. Additionally, in order to locate any platinum-group minerals (PGM), six of the polished thin sections were automatically searched by electron microprobe (Cameca SX50) on a 1- or 2- $\mu\text{m}$  grid, using the back-scattered electron signal to locate minerals with high atomic number. The PGM found were characterised using energy-dispersive spectra (EDS) and, if possible, wavelength-dispersive analysis (WDS) operating at 15 kV and 20 nA.

## **Petrography**

Petrographic study of the chromitite samples recorded between 5-10% interstitial silicate minerals in the ultramafic lithologies. In chromitite sample LGR 013 this consists largely of olivine with minor alteration to serpentine, whilst the other samples are more altered with mainly serpentine, chlorite and a few remnants of olivine. A photomicrograph of chromitite LGR 010 showing olivine with minor serpentine alteration is shown in Figure 13. The chromite itself is generally fresh showing red to red-brown colours with some minor darkening along fractures, but LGR 001 (chromitite) is much more intensely darkened indicating alteration to 'ferrit-chromite' and magnetite. Several of the chromitite samples have been thinly veined by carbonate.

The dunites are very fresh with only minor serpentinisation along cracks. They contain around 1% chromite and interstitial pyroxene which in one sample (LGR 002) is clinopyroxene, and the other (LGR 012) orthopyroxene. One dunite sample (LGR 012) contains around 5% orthopyroxene trending towards harzburgite in composition, and is cut by narrow zones of cataclasite, which are notable for the lack of retrograde alteration (Figure 14).

Sample LGR 009 (peridotite) contains abundant olivine with around 25% orthopyroxene and 5% clinopyroxene (Figure 15). Although this is classified as a peridotite, it could be similar to those previously described by Siebrat<sup>42</sup> as Iherzolite.

This sample also contains minor chromite and slight alteration to serpentine and chlorite.

Three samples of pyroxenite were examined, LGR 005, LGR 006, and LGR 014. Samples LGR 006 and LGR 014 are almost entirely orthopyroxene with a little interstitial clinopyroxene and traces of olivine, whilst LGR 005 contains approximately 15% clinopyroxene and is classified as websterite (Figure 16). The pyroxenites are generally very fresh but LGR 005 has slight amphibolitisation and LGR 014 is cut by zones of talc alteration.

In general, the samples examined are all very fresh, and none show the typical porphyroclastic mantle tectonite fabric that characterises ophiolitic mantle rocks. This suggests that they are part of the magmatic suite of the Mantle Transition Zone (MTZ).

### **Occurrence of PGM**

PGM were found in two of the samples studied. In the dunite sample LGR 012, an 8  $\mu\text{m}$  grain of native Pt (with minor Fe) was identified in association with fine-grained serpentinisation of the olivine (Figure 17 A). The second observed occurrence, in chromitite LGR 013, is a 10  $\mu\text{m}$  grain of Ru-Ir alloy along a Cr-spinel-chlorite grain boundary (Figure 17 B).

The presence of PGM associated with alteration minerals serpentinite and chlorite suggests possible remobilisation of the PGM during alteration of the host lithology.

## **Lithogeochemical studies**

### **Methodology - Major and trace elements**

Eight samples representing the different lithologies present at localities C1 and C2 were analysed for major and trace elements by Wavelength Dispersive X-Ray Fluorescence Spectrometry (WD-XRFS) using fused glass beads. The samples were dried overnight at 105°C and pre-ignited at 1050°C before analysis. Loss on ignition (LOI) was determined after 1 hour at 1050°C. The results of these analyses are shown in Table 1.

Thirteen samples from C1 and C2, comprising five chromitites, four dunites, two pyroxenites, one peridotite and one sample of microgabbro, were crushed and milled in the BGS labs in the UK. Representative sub-samples were analysed by ACME Analytical Laboratories in Canada for gold and the PPGE (Pt, Pd and Rh). Thirty gram samples underwent lead-collection fire-assay fusion for total sample decomposition, followed by acid digestion of the silver doré bead and ICP-MS analysis.

Representative sub-samples of five samples from C1 and C2, three dunites, two chromitites and one peridotite, were analysed for five PGE (Pt, Pd, Rh, Ru and Ir) by nickel sulphide fire assay at Cardiff University based on the method used by McDonald and Viljoen<sup>28</sup>.

### **Results - Major elements**

The major element analyses of the ultramafic rocks are shown in Table 1. This shows compositions typical of ultramafic rocks with all samples having high MgO, low SiO<sub>2</sub>, and high MgO/(FeO + MgO) ratios. The pyroxenites have much higher SiO<sub>2</sub> and lower MgO, while the samples containing more clinopyroxene contain higher CaO. In general, the samples have a low level of serpentinisation, indicated by the low LOI. However, two of the samples, LGR008 and LGR009, a dunite and peridotite, have relatively high LOI which suggests a higher level of serpentinisation.

### **Results - PGE and PGM**

Platinum-group element concentrations in the Logar samples are shown in Table 3. The concentrations of PGE in the chromitites are very low with maxima of 6.5 ppb Pt and 5.5 ppb Pd. Rh values are relatively high, with two samples exceeding 10 ppb. In dunites, Pt and Pd values are generally <10 ppb, although sample LGR 012 (from C2) contains the maximum reported values of 11.3 ppb Pt and 9.4 ppb Pd. The pyroxenite samples have relatively high Pt values with an average of 13 ppb whilst they have very low Pd and Rh values. In dunites, sample LGR 012 from quarry C2 records higher values for most PGE than the other dunite samples. The Pt and Pd values are more variable, ranging from 5-11 ppb Pt and 2-10 ppb Pd. In general Rh, Ir and Ru

values are also low with a maximum of 8 ppb Ru. However, these observations are based on limited data and further sampling would be needed to identify any significant patterns in the data.

The chondrite-normalised data for the five PGE determined at Cardiff University are shown in Figure 18. The plot of the Logar data shows two clear trends: (i) the two chromitites (LGR 003 and LGR 013) have marked positive Ru anomalies, Pt negative anomalies and a generally negative slope: (ii) one of the dunites (LGR 012) and the peridotite (LGR 009) have no negative Pt anomaly, relatively enriched in the low temperature PGEs, Pd and Au, and show only a very slight Ru anomaly with positive slopes. This suggests that the two rock groups may have different origins for their PGE. Data from the UAE ophiolite<sup>14</sup> and the Zambales ophiolite<sup>9</sup> are included in Figure 18 for comparison.

## **Mineral chemistry**

### **Methodology**

Analyses of chromites and silicate minerals were undertaken at the Department of Electron Microanalysis at the State Geological Institute of Dionýz Štúr in Bratislava, Slovakia. This work was carried out on a Cameca SX-100 electron microprobe with an accelerating voltage of 15 kV (20 kV for sulphides) and sample current of 20 nA. The elements were calibrated using synthetic or natural standards: Si-SiO<sub>2</sub>, Ti-TiO<sub>2</sub>, Al-Al<sub>2</sub>O<sub>3</sub>, Cr-Cr<sub>2</sub>O<sub>3</sub>, Fe-fayalite, Mn-rhodonite, Ni-Ni, Mg-MgO, Ca-wollastonite, Na-albite, K-orthoclase, Zr-zircon, S-chalcopyrite and Zn-willemitte. A small number of other WDS analyses were also performed at the BGS (on chlorite and Cr-spinel) to augment and validate the work carried out in Slovakia. There is good agreement between both sets of results.

### **Results – Major elements**

The analyses of typical chromites are shown in Table 2. These show that the chromitites from C1 and chromites in dunites from both C1 and C2 have high Cr# (Cr/Cr+Al) values around 0.8 up to over 0.9 in LGR 001. The chromitites from C2 have much lower values 0.55- 0.7. The orthopyroxenite (LGR 006) has intermediate values around 0.7, similar to the top of the range of C2 chromitites. The data also

shows a considerable variation in  $\text{Al}_2\text{O}_3$  between C1 and C2, with samples from C1 recording up to 14%  $\text{Al}_2\text{O}_3$  and samples from C2 recording up to 25%  $\text{Al}_2\text{O}_3$ . In addition, there are also variations in the content of  $\text{Cr}_2\text{O}_3$ , FeO and MgO within the samples. This suggests that samples from C1 were formed in a different environment to C2 (discussed later).

The dunites and chromitites have very magnesian olivines in the range  $\text{Fo}_{92-96}$ , while the orthopyroxenite has  $\text{Fo}_{88.5}$  and the pyroxene is  $\text{En}_{90}$  less magnesian than the dunites and chromitites. The microgabbro has clinopyroxene with Mg# 67-74 and plagioclase mostly around  $\text{An}_{68}$  but some  $\text{An}_{50}$ .

## Discussion

PGE are frequently associated with podiform chromitites in the mantle and the Mantle Transition Zone (MTZ). The concentration of PGE in most chromitites in ophiolites is generally low and the majority do not contain above 500 ppb<sup>27</sup>. The concentration of PGE in the chromitites studied from Logar are comparable with those in most ophiolites around the world. However, several ophiolites are known with high PGE contents. For example, the Tropoja and Bulqiza ophiolite complexes in Albania have recorded up to 800 ppb Pt+Pd in chromitites from the upper part of the mantle<sup>31</sup>. Chromitites from the Semail ophiolite, Oman, are also known to contain up to 1 500 ppb PGE<sup>2</sup>, whilst chromitites from the Hochgrössen and Kraubath massifs, Austria, have recorded up to 2 269 ppb combined PGE, including 940 ppb Pt<sup>45</sup>.

Chromitites from ophiolites are usually characterised by negatively sloping chondrite-normalised PGE patterns relatively enriched in the IPGE (Ir, Ru and Rh) e.g. the Semail ophiolite, Oman<sup>32</sup>, the Troodos ophiolite, Cyprus<sup>36</sup>, the Bou Azzer ophiolite, Morocco<sup>19</sup>, and the Veria ophiolite complex, Greece<sup>46</sup>. However, ophiolites that are relatively enriched in Pt and Pd and characterised by positively sloping chondrite-normalised PGE patterns are also known e.g. at Unst<sup>35</sup>, Portugal<sup>12</sup> and in the Urals<sup>50</sup>. However, these are rare and, at Unst, the enrichment is probably caused by localised hydrothermal remobilisation of the PGE<sup>20</sup>, although other researchers have stressed the major importance of magmatic processes at this location<sup>35</sup>.

The Semail ophiolite, Oman contains relatively high PGE values, up to 1 500 ppb, in chromitites in the mantle and other ultramafic rocks in veins cutting the mantle and the Mixed Unit<sup>3</sup>. The rocks containing these high PGE values are all associated with the second stage Supra Subduction Zone (SSZ) hydrous magmatic phase. More recent studies<sup>38</sup>, have reported high values of both IPGE (50-275 ppb) and PPGE (50-515 ppb) in pyroxenites, wehrlites and chromites from the UAE ophiolite. These are formed during a late magmatic phase and could be broadly similar to the late pyroxenites at Logar.

PGM are widely recorded in ophiolites worldwide e.g. the Zambales ophiolite, Philippines<sup>9</sup>, Troodos ophiolite, Cyprus<sup>36</sup>, the Kop mountains, Turkey<sup>47</sup>, Vourinos<sup>24</sup>, and Pindos<sup>44</sup>, many others not cited here. The occurrence of PGM from the LOC, a grain of native platinum in a dunite and a Ru-Ir alloy in a chromitite, is therefore not surprising given previous discoveries in other ophiolites e.g the Unst ophiolite, Shetland<sup>35</sup>, Bou Azzer ophiolite, Morocco<sup>19</sup>, and the Kempirsai ophiolite complex, Urals<sup>17</sup>. However, this study represents the first time that PGM have been identified within ultramafic rocks from the LOC in Afghanistan.

The association of these PGM with serpentinised and altered olivine and spinel crystal boundaries suggests some remobilisation of PGM during the serpentinisation of the host rock. No evidence of any primary sulphides was observed. However, since only limited sampling of the LOC was carried out during this study, further investigations would be necessary to fully understand the distribution of PGM in the LOC.

### **Petrogenesis of the Logar ophiolite**

The compositions of chromite and chrome-spinel grains are useful indicators of petrogenetic conditions in the mantle. Chrome-spinel is highly sensitive to the degree of partial melting in mantle peridotites and has been widely used for the tectonic discrimination of mafic and ultramafic rocks<sup>6, 11, 16</sup>. The geochemistry of chrome-spinel in mantle peridotites provides information on both the residual mantle, such as its degree of melting and condition of melting, and on the nature and extent of melt/rock interaction<sup>51, 25</sup>. This information can be used to determine whether the mantle sequence has a Mid-Ocean Ridge (MOR) setting or a Supra-Subduction Zone (SSZ) origin, or those that have formed from more than one tectonic setting<sup>33, 34</sup>.

In addition, the Ti content of chrome-spinel is a reliable indicator of magma chemistry because the diffusivity of  $Ti^{4+}$  in olivine is low<sup>40</sup>.  $TiO_2$  is also sensitive to melt-rock reaction and can fingerprint melt composition<sup>34</sup>. Data for the LOC in Table 3 show very low Ti levels with high Cr# from 0.5 to nearly 1.0. The plot of Cr# against  $TiO_2$  in spinel (Figure 19) shows different compositional ranges for chromites from the two quarries. The chromites from C2 have lower Cr# 0.5-0.6 with a wide range of  $TiO_2$  values. This is typical of chromitites from MOR-type magmas<sup>26</sup>. Chromitites from C1 have a much higher Cr# and a narrower range of  $TiO_2$  values. This suggests formation from, or reaction with, boninitic magmas in a supra-subduction zone environment<sup>26</sup>.

The plot of Cr# against Fo (olivine) (Figure 20) also highlights the differences between C1 and C2. The Cr#-Fo diagram is effective for distinguishing between residual mantle peridotites and peridotites formed by fractional crystallization<sup>6,7</sup>. Both Cr# of spinel and Fo content of olivine increase during partial melting and form the Olivine-Spinel Mantle Array (OSMA) (see Figure 20) within which residual peridotites predominantly plot<sup>6</sup>. In contrast, spinels from lavas have lower Fo and so plot to the right of the OSMA trend because the Fo content of olivine decreases during fractional crystallisation<sup>7</sup>. The Cr#-Fo fractionation trend is dependent on the phases co-crystallising with spinel: Cr# decreases upon crystallisation of chrome-spinel with olivine and pyroxene but Cr# increases upon crystallisation of chrome-spinel with plagioclase<sup>7</sup>. Extrapolation of the Cr#-Fo fractionation line back to the OSMA trend enables the compositions of the mantle residue in equilibrium with the primary magma to be estimated<sup>7</sup>.

The Cr# values are higher in C1 than C2 but have similar Fo values. The dunites have high Cr# but slightly lower Fo, and the pyroxenite has both lower Cr# and lower Fo. When these compositions are compared with those from the mantle array it shows that the pyroxenite falls on the low Fo side indicating some fractional crystallisation, while the chromitites fall to the high Fo side suggesting a residual nature. The dunites fall within the mantle array with compositions suggesting high degrees of partial melting consistent with boninitic magmas from a SSZ setting. The two trends of chondrite-normalised PGE data for the Logar data also support the hypothesis that the different rock types in the LOC have different origins for their PGE. Since both trends are

present in the same place, this could mean that more than one phase of mineralisation operated here.

Logar data are broadly comparable in terms of Cr# and TiO<sub>2</sub> to those described from the UAE<sup>14</sup> and northern Oman<sup>39</sup>.

It is interesting that these chromites of contrasting composition are found relatively close together; quarries C1 and C2 are within a few hundred metres of each other. This may suggest that the two types of chromitites are formed as the product of two discrete mantle melting events. Some residual chromitites may have formed from an early MOR phase of magmatism with later boninitic melts having reacted with the mantle to form the SSZ type chromitites in other areas. This is similar to the theory proposed for the origin of two chromitite pods 200 m apart in northern Oman<sup>2</sup>.

Magma producing chromitites similar to those seen at C1 tend to be S-undersaturated, Ti-poor, PGE-enriched, have a high Cr# and are boninitic in composition<sup>14, 22, 10, 37</sup>. Magma of this type is formed from widespread fluid-induced melting of previously melted lithospheric mantle beneath an arc<sup>22</sup>. These boninitic magmas would rise and react with uppermost mantle harzburgite to form high Cr# (>50% Cr<sub>2</sub>O<sub>3</sub>) chromitites in dunite pods<sup>52</sup>. The formation of chromite in supra-subduction zones is illustrated in Figure 21.

Magma producing chromitites similar to those seen at C2 tend to be S-saturated, PGE-poor, with a low Cr # and a wide range of TiO<sub>2</sub> value<sup>14, 22, 10, 37</sup>. Magma of this type is produced in a fast-spreading mid-ocean ridge environment.

It is important to stress that our observations are based on limited sampling and analysis. Further sampling would be necessary to determine whether these samples are representative of the LOC, and to better understand the petrogenetic and metallogenic processes operating at the ophiolite complex.

## Conclusions

This study has identified PGM for the first time from the Logar Ophiolite Complex in Afghanistan. No modern work has been undertaken on the tectonic setting of the LOC and it was not the purpose of this study to investigate this further. However, field observations presented in this study, together with the analysis of a limited number of samples, suggest that the chromitites in the LOC appear to originate from two different sources. One end-member is a melt derived from a low Cr #, PGE-poor MOR environment whilst the other is from a high Cr#, relatively PGE-rich boninitic magma produced in a SSZ setting.

The mineralogical relationship of the PGM identified in this study indicates that the PGM may have been remobilised.

## Acknowledgements

The work undertaken in this study has been completed as a part of a DfID-funded British Geological Survey project, “Institutional Strengthening of the Afghan Geological Survey”, and is published with permission of the Executive Director, British Geological Survey. The authors gratefully acknowledge the assistance of many staff at the Afghan Geological Survey and Ministry of Mines and Industry, including Minister Ibrahim Adel and Deputy President of AGS Eng. Omar. The comments and discussions with Tim Colman and Stan Coats, both formerly of BGS, are also greatly appreciated. In addition, Stan Coats generously provided several of the figures for this work.

## References

1. Sh. Abdullah, and V. M. Chmyrev (Editors-in-chief): *Geology and Mineral Resources of Afghanistan*, Report 602, Afghanistan Geological Survey Archive, Kabul, 1980.
2. A. H. Ahmed and S. Arai: Unexpectedly high-PGE chromitite from the deeper mantle section of the northern Oman ophiolite and its tectonic implications. *Contrib. Mineral. Petrol.*, 2002, **143**, 263-278.
3. A. H. Ahmed and S. Arai: Platinum-group minerals in podiform chromitites of the Oman ophiolite. *Canadian Mineralogist*, 2003, **41**, 597-616.

4. E. Anders and N. Grevesse. Abundances of the elements: Meteoric and solar. *Geochimica et Cosmochimica Acta*, 1989, **53**, 197-214.
5. G. Andritzky: Das Kristallinim Gebiet Panjao – Kabul – Jalalabad (Zentral- und Ost-Afghanistan). Kabul. *Beih. Geol. Jb*, 1970, **96**, 5-82 (in German).
6. S. Arai: Characterization of spinel peridotites by olivine-spinel compositional relationships: Review and interpretation. *Chemical Geology*, 1994a, **113**, 191-204.
7. S. Arai: Compositional variation of olivine-chromian spinel in Mg-rich magmas as a guide to their residual spinel peridotites. *Journal of Volcanology and Geothermal Research*, 1994b, **59** (4), 279-293.
8. T. Augé. Platinum-group mineral inclusions in ophiolitic chromitite from the Vourinos complex, Greece. *Canadian Mineralogist*, **23**, 1985, 163–171.
9. G. C. Bacuta, R. W. Kay, A. K. Gibbs, and B. R. Lippin: Platinum-group element abundance and distribution in chromite deposits of the Acoje Block, Zambales Ophiolite Complex, Philippines. *J. Geochem. Expl.*, 1990, **37**, 113-145.
10. S. J. Barnes. Are Bushveld U-type parent magmas boninites or contaminated komatiites? *Contributions to Mineralogy and Petrology*, 1989, 101, 447-457.
11. S.J. Barnes and P.L. Roeder: The range of spinel compositions in terrestrial mafic and ultramafic rocks, *J. Petrol.* 2001, 42, 2279–2302.
12. J. C. Bridges, H. M. Prichard, C. R Neary, and C. A. Meireles: Platinum-group element mineralization in chromite-rich rocks of Braganca massif, northern Portugal. *Trans Inst Min Metall B*, 1994, 102, 103–113.
13. V. M. Chmyrev, V. I. Dronov, K. F. Stazhilo-Alekseyev, A. Kh. Kafarskiy, E. P. Malyarov, and I. M. Sborshchikov: Geological structure and mineral resources of Afghanistan. 1977. Afghanistan Geological Survey, Kabul (in Russian).
14. S. A. S. Dare: Chrome-spinel geochemistry of the northern Oman-United Arab Emirates ophiolite, PhD thesis (unpublished), Cardiff University, Wales, UK, 2008.
15. Sh. Sh. Denikaev, I. V. Pyzhyanov, V. P. Feoktistov, A. Adzhrauddin, Sh. N. Nurbayev and J. M. Konev: The Geology and Minerals of the Southern Part of Eastern Afghanistan (Preliminary report of the Kabul group for 1970). 1971. Unpublished report, Afghanistan Geological Survey Archive, Kabul,

Afghanistan.

16. H. J. Dick and T. Bullen: Chromian spinel as a petrogenetic indicator in abyssal and alpine-type peridotites and spatially associated lavas. *Contributions to Mineralogy and Petrology*, 1984, **86**, 54-76.
17. V. V. Distler, V. V. Kryachko and M. A. Yudovskaya: Ore petrology of chromite-PGE mineralisation in the Kempirsai ophiolite complex. *Mineralogy and Petrology*, 2008, **92**, 31-58.
18. V. I. Dronov, K. F. Stazhilo-Alekseev, A. Ya Kotchetkov, S. S. Karapetov, S. M. Kalimulin and I. I. Sonin: The Geology and Minerals of Central and South-Western Afghanistan. Afghanistan Geological Survey Archive, Kabul, Afghanistan (in Russian).
19. M. El Ghorfi, F. Melcher, T. Oberthür, A. E. Boukhari, L. Maacha, A. Maddi, and M. Mhaili: Platinum group minerals in podiform chromitites of the Bou Azzer ophiolite, Anti Atlas, Central Morocco. *Mineralogy and Petrology*, 2008, **92**, 59-80.
20. A. G. Gunn: Drainage and overburden geochemistry in exploration for platinum-group element mineralisation in the Unst ophiolite, Shetland, U.K. *Journal of Geochemical Exploration*, 1989, **31**, 209-236.
21. A. S. Hafisi: Geologisch petrografische Untersuchung des chromitführenden ultrabazitmassivs vom Logar Tal (sudostlich von Kabul). 1974. Afghanistan Geological Survey Archive, Kabul, Afghanistan (in German).
22. P. Hamlyn and R. Keays: Sulfur saturation and second-stage melts: application to the Bushveld platinum metal deposits. *Economic Geology*, 1986, **81**, 1431-1449.
23. D. Jouselin and A. Nicolas: The Moho transition zone in the Oman ophiolite - relation with wehrlites in the crust and dunites in the mantle. *Marine Geophysical Researches*, 2000, **21**, 229-241.
24. A. Kapsiotis, T.A. Grammatikopoulos, F. Zaccarini, B. Tsikouras, G. Garuti, K. Hatzipanagiotou. Platinum-group mineral characterisation in concentrates from low-grade PGE chromitites from the Vourinos ophiolite complex, northern Greece. *Trans. Inst. Min. Metall. B*, 2006, **115** (2), 49-57(9).
25. P. B. Kelemen, N. Shimizu and V. J. M. Slaters: Extraction of mid-ocean-ridge basalt from the upwelling mantle by focused flow of melt in dunite channels. *Nature*, 1995, **375**, 747 – 753.

26. V. S. Kamenetsky, A. J. Crawford and S. Meffre: Factors controlling chemistry of magmatic spinel: an empirical study of associated olivine, Cr-spinel and melt inclusions from primitive rocks. *J. Petrol.*, 2001, **42**, 655–671.
27. M. LeBlanc: Platinum-group elements and gold in ophiolitic complexes: distribution and fractionation from mantle to oceanic floor. *In Ophiolite Genesis and Evolution of the Oceanic Lithosphere, Oman* (T. Peters *et al.*, eds.), 1991, Kluwer, Dordrecht, The Netherlands, 231-260.
28. I. McDonald and K. S. Viljoen: Platinum-group element geochemistry of mantle eclogites. *Applied Earth Science (Trans. Inst. Min. Metall. B)*, 2006, **115**, No. 3, 81-93.
29. E. B. Nevretdinov, L. V. Kubatkin, and Sh. Abdullah: Relation of Logar ultramafic rocks and rocks of the Kabul Massif. *Workshop Proceedings*, 1978, Kabul, 12-18 (in Russian).
30. E. B. Nevretdinov and M. Mirzamon: Report on prospecting - survey and evaluation works on asbestos, chromite and other raw material in the northern part of the Logar Ultramafic Massif in 1978. 1979, Afghanistan Geological Survey Archive, Kabul, Afghanistan (in Russian).
31. M. Ohnenstetter, N. Karaj, A. Neziraj, Z. Johan and A. Cina: Le potentiel platinifère des ophiolites: minéralisations en éléments du groupe du platine (PGE) dans les massifs de Tropoja et Bulquiza, Albanie. *C.R. Acad. Sci. Paris*, 1991, **13**, Sér. **II**, 201-208 (in French).
32. N. J. Page, J. S. Pallister, M. A. Brown, J. D. Smewing and J. Haffy: Palladium, platinum, rhodium, iridium and ruthenium in chromite-rich rocks from the Semail Ophiolite, Oman. *Canadian Mineralogist*, 1982, **20**, 537-548.
33. J. Parkinson and J. Pearce: Peridotites from the Izu-Bonin-Mariana Forearc (ODP Leg 125): Evidence for Mantle Melting and Melt-Mantle Interaction in a Supra-Subduction Zone Setting. *Journal of Petrology*, 1998, **39**, 1577-1618.
34. J. Pearce, P. F. Barker, S. J. Edwards, I. J. Parkinson and P. T. Leat: Geochemistry and tectonic significance of peridotites from the South Sandwich arc-basin system, South Atlantic. *Contributions to Mineralogy and Petrology*, 2000, **139**, 36-53.
35. H. M. Prichard, P. J. Potts and C. R. Neary: Platinum group element minerals in the Unst chromite, Shetland Isles. *Trans. Inst. Min. Metall. B*, 1981, **90**, B186-188.

36. H. M. Prichard and R. A. Lord: Platinum and Palladium in the Troodos Ophiolite Complex, Cyprus. *Canadian Mineralogist*, 1990, **28**, 607-617.
37. H. M. Prichard, R. A. Lord, and C. R. Neary. A model to explain the occurrence of platinum- and palladium-rich ophiolite complexes. *Journal of the Geological Society*, 1996, **153**, 323-328.
38. N. S. Robins, A. J. Benham and C. J. Mitchell: The Geology and Geophysics of the United Arab Emirates. Volume 3: Economic Geology and Hydrogeology, Keyworth, Nottingham: British Geological Survey, 2006.
39. H. Rollinson: The geochemistry of mantle chromitites from the northern part of the Oman ophiolite: inferred parental melt compositions. *Contrib. Mineral. Petrol.*, 2008, **156**, 273-288.
40. P. A. H. Scowen, P. L. Roeder, and R. T. Heltz: Reequilibration of chromite within Kilauea Iki lava lake, Hawaii. *Contrib. Mineral. Petrol.*, 1991, **107**, 8-20.
41. H. G. Siebdrat: Parallelisierung von optisch ermittelter und analytisch berechneter Mineralzusammensetzung bei Chromiterzen Afghanistans. *Bergbauwissenschaften Jb.*, 1965, **12**, H. ½, 28-34 (in German).
42. H. G. Siebdrat: Chromite in ultrabasischen Magmatiten des unteren Logar-Tales (Sudost-Afghanistan). *Beih. Geol. Jb.*, 1971, **96**, 209-226 (in German).
43. A. Shareq, V. N. Voinov, E. B. Nevretdinov, L. V. Kubatkin and I. A. Gusav: The Logar ultrabasite massif and its reflection in the magnetic field (East Afghanistan). *Tectonophysics*, 1980, **62**, 1-5.
44. M. Tarkian, M. Economou-Eliopoulos, and G. Sambanis. Platinum group minerals in chromitites from the Pindos ophiolite complex, Greece: *Neues Jahrbuecher fur Mineralogic Monatshefte*, 1996, **10**, 145-160.
45. O. A. R. Thalhammer, W. Prochaska and H. W. Mühlans: Solid inclusion in chrome-spinels and platinum-group element concentration from the Hochgrössen and Kraubath ultramafic massifs (Austria). *Contrib. Mineral. Petrol.*, 1990, **105**, 66-80.
46. G. Tsoupas and M. Economou-Eliopoulos: High PGE contents and extremely abundant PGE-minerals hosted in chromitites from the Veria ophiolite complex, northern Greece. *Ore Geology Reviews*, 2008, **33**, 3-19.

47. M. Uysal, M. Tarkian, B. Sadiklar and C. Şen: Platinum-group-element geochemistry and mineralogy of ophiolitic chromitites from the Kop Mountains, northeastern Turkey. *Canadian Mineralogist*, 2007, **45**, 355-377.
48. M. E. Volin: Chromite deposits in Logar Valley, Kabul Province. United States Bureau of Mines, 48, Afghanistan Geological Survey, Kabul, 1950.
49. D. Wirtz: Zur regional-geologischen Stellung der Afghanischen Gebirge. *B.geol. Jb., Hannover*, 1964, **70**, 5-18 (in German).
50. F. Zaccarini, E. Pushkarev and G. Garuti: Platinum-group element mineralogy and geochemistry of chromitite of the Kluchevskoy ophiolite complex, central Urals (Russia). *Ore Geology Reviews*, 2008, **33**, 20-30.
51. M. F. Zhou, P. T. Robinson and W. J. Bai: Formation of podiform chromites by melt/rock interaction in the upper mantle. *Mineralium Deposita*, 1994, **29**, 98-101.
52. M. F. Zhou, M. Sun, R. R. Keays and R. W. Kerrich: Controls on platinum-group elemental distributions of podiform chromitites: a case study of high-Cr and high-Al chromitites from Chinese orogenic belts. *Geochim. Cosmochim. Acta*, 1998, **62**, 677-688.

Diagrams:

Figure 1. The location of the Logar Ophiolite Complex in Afghanistan.

Figure 2. Simplified tectonic map of Afghanistan showing the different terranes in the country.

Figure 3. Satellite interpretation of the tectonic setting of the Logar Ophiolite Complex based on Landsat imagery.

Figure 4. Lithological section through the Ultramafic Complex and Pillow Lava Complex of the Logar Ophiolite Complex. (Modified after Nevretdinov and Mirzamon<sup>30</sup>).

Figure 5. View looking north across the ultramafic part of the LOC. A dyke of microgabbro composition can be seen trending north-west in the mid-background.

Figure 6. Location of chromite quarries visited, other reported chromite localities and simplified geology of the Logar Ophiolite Complex. Modified from Siebrat<sup>42</sup>.

Figure 7. First chromite quarry (C1) visited in the Logar Ophiolite Complex (34° 13' 6.4" N, 69° 2' 29.1" E) looking west.

Figure 8. Massive chromitite in the side of the C1 chromite quarry (34° 13' 16.3" N, 69° 2' 28.6" E)

Figure 9. Disseminated chromite and blebs of chromite associated with carbonate veins in dunite from the C1 chromite quarry (34° 13' 16.3" N, 69° 2' 28.6" E)

Figure 10. Sub-massive chromite mineralisation taken from the C1 quarry (34° 13' 17.7" N, 69° 2' 28.2" E)

Figure 11. Discordant pyroxenite body (grey) within dunite host (brown) occurring at the western end of the C1 chromite quarry (34° 13' 17.7" N, 69° 2' 28.2" E)

Figure 12. Second quarry (C2) visited in the Logar Ophiolite Complex (34° 13' 43.6" N, 69° 1' 34.3" E). Lithologies exposed in the quarry wall include pyroxenite (grey), dunite (brown), and carbonitised ultramafic rocks (white)

Figure 13. SEM photomicrograph of LGR 010 (chromitite) from C1 showing interlocking chromite crystals (white) and interstitial olivine (light grey) being replaced by serpentine (lizardite) (dark-grey).

Figure 14. Photomicrograph of dunite (LGR 012) in plane polarised light. Note cataclasite zone of crushed olivine through the sample. Scale bar 2 mm.

Figure 15. Photomicrograph of peridotite (LGR 009) in cross polarised light. The olivine (highly coloured) is very fresh and comparatively unaltered. Note the opaque chromite inclusions (black). Scale bar 2 mm.

Figure 16. Photomicrograph of LGR 005 (pyroxenite - websterite) in cross polarised light showing typically fresh, unaltered diopside crystals. Scale bar 2 mm.

Figure 17 A) Sample LGR 012 (dunite), a grain of native Pt (+Fe) found associated with serpentinised olivine, and, B) Sample LGR 013 (chromitite), a grain of Ru-Ir alloy found along an altered olivine/Cr-spinel boundary.

Figure 18. Chondrite-normalised plots of samples from C1 and C2. Chondrite PGE levels from Anders and Grevesse<sup>4</sup>. UAE data taken from Dare (pers. comm.), Zambales data from Bacuta et al<sup>9</sup>.

Figure 19. Cr# ( $\text{Cr}/(\text{Cr} + \text{Al})$ ) and  $\text{TiO}_2$  of chromite samples from the LOC.

Figure 20. Cr# spinel against olivine Fo content for rock samples taken from C1 and C2. The diagram shows the olivine-spinel mantle array (OSMA) and melting trend (annotated by % melting) of Arai<sup>6</sup> and the fractional crystallization trend to lower Fo<sup>7</sup>.

Figure 21. Model for the formation of podiform chromite deposits in a supra-subduction zone.



Sample name	Lithology	SiO <sub>2</sub>	TiO <sub>2</sub>	Al <sub>2</sub> O <sub>3</sub>	Fe <sub>2</sub> O <sub>3t</sub>	Mn <sub>3</sub> O <sub>4</sub>	MgO	CaO	Na <sub>2</sub> O	K <sub>2</sub> O	P <sub>2</sub> O <sub>5</sub>	SO <sub>3</sub>	Cr <sub>2</sub> O <sub>3</sub>	SrO	ZrO <sub>2</sub>	BaO	NiO	CuO	ZnO	PbO	LOI	Total	
		%	%	%	%	%	%	%	%	%	%	%	%	%	%	%	%	%	%	%	%	%	%
LGR002	Dunite	40.95	<0.01	0.16	8.50	0.13	47.89	0.33	n.d.	n.d.	n.d.	n.d.	0.78	n.d.	n.d.	n.d.	0.40	n.d.	n.d.	n.d.	1.83	100.97	
LGR004	Dunite	43.52	<0.01	0.29	8.54	0.14	45.04	0.61	n.d.	n.d.	n.d.	n.d.	0.53	n.d.	n.d.	n.d.	0.32	n.d.	n.d.	n.d.	1.97	100.96	
LGR005	Pyroxenite	56.55	0.02	0.84	7.25	0.16	33.61	1.42	n.d.	n.d.	n.d.	n.d.	0.54	n.d.	n.d.	n.d.	0.10	n.d.	n.d.	n.d.	0.49	100.98	
LGR006	Pyroxenite	52.85	0.02	0.74	7.67	0.16	36.10	1.23	n.d.	n.d.	n.d.	n.d.	0.53	n.d.	n.d.	n.d.	0.16	n.d.	n.d.	n.d.	1.39	100.85	
LGR008	Dunite	39.20	<0.01	0.17	9.02	0.13	45.41	0.27	n.d.	n.d.	n.d.	n.d.	0.48	n.d.	n.d.	n.d.	0.34	n.d.	n.d.	n.d.	5.83	100.85	
LGR009	Peridotite	41.73	<0.01	0.26	8.44	0.14	43.16	0.65	n.d.	n.d.	n.d.	n.d.	0.43	n.d.	n.d.	n.d.	0.30	n.d.	n.d.	n.d.	5.87	100.98	
LGR012	Dunite	43.10	<0.01	0.37	8.63	0.14	46.18	0.46	n.d.	n.d.	n.d.	n.d.	0.42	n.d.	n.d.	n.d.	0.32	n.d.	n.d.	n.d.	1.34	100.96	
LGR014	Pyroxenite	55.73	0.03	1.04	7.70	0.17	32.71	1.55	n.d.	n.d.	n.d.	n.d.	0.55	n.d.	n.d.	n.d.	0.10	n.d.	n.d.	n.d.	0.96	100.54	

Table 1. Major and trace element analyses of dunites, peridotites and pyroxenites from the Logar Ophiolite Complex. Analysis by Wavelength Dispersive X-Ray Fluorescence Spectrometry (WD-XRFS) using fused glass beads at the British Geological Survey, UK. Fe<sub>2</sub>O<sub>3t</sub> represents total iron expressed as Fe<sub>2</sub>O<sub>3</sub>. SO<sub>3</sub> represents sulphur retained in the fused bead after fusion at 1200°C. n.d. = not detected (below detection limit)

Sample no.	Lithology	Location	SiO <sub>2</sub>	TiO <sub>2</sub>	Al <sub>2</sub> O <sub>3</sub>	Cr <sub>2</sub> O <sub>3</sub>	Fe <sub>2</sub> O <sub>3</sub>	FeO <sup>a</sup>	MnO	MgO	CaO	NiO	ZnO	Cr# (Cr/Cr+Al)	Total
LGR01.1	Chromitite	C1	0.11	0.14	8.66	60.23	3.55	12.4	0.42	13.36	0	0.04	0	0.823	98.91
LGR01.2	Chromitite	C1	0.01	0.13	8.98	60.64	3.62	12	0.37	13.69	0	0.11	0	0.819	99.53
LGR01.3	Chromitite	C1	0.02	0.13	8.81	60.72	3.62	12.23	0.38	13.52	0	0.1	0	0.822	99.51
LGR01.5	Chromitite	C1	0.03	0.16	2.72	63.53	5.22	14.71	0.46	10.9	0	0.03	0.04	0.940	97.78
LGR01.6	Chromitite	C1	0.01	0.15	2.52	63.34	5.36	15.6	0.49	10.23	0.01	0.09	0	0.944	97.79
LGR01.7	Chromitite	C1	0.01	0.17	2.68	63.46	4.7	17.21	0.34	9.36	0	0.02	0.08	0.941	98.02
LGR01.14	Chromitite	C1	0.03	0.14	8.82	60.14	3.58	11.87	0.31	13.66	0.01	0.05	0	0.821	98.59
LGR02.1	Dunite	C1	0	0.15	9.37	57.81	4.85	16.81	0.41	10.65	0	0.02	0.16	0.805	100.25
LGR02.2	Dunite	C1	0.02	0.14	9.35	57.83	4.49	16.87	0.46	10.52	0.03	0.06	0.07	0.806	99.83
LGR02.3	Dunite	C1	0.03	0.14	9.34	57.21	4.82	16.92	0.45	10.45	0	0.08	0.04	0.804	99.45
LGR02.4	Dunite	C1	0.03	0.14	9.68	54.79	5.6	19.25	0.51	8.82	0.01	0	0.06	0.792	98.89
LGR02.5	Dunite	C1	0	0.13	9.15	57.97	4.81	16.57	0.48	10.66	0.01	0.03	0.17	0.810	99.97
LGR02.7	Dunite	C1	0.03	0.09	8.63	58.6	4.4	17.22	0.48	10.18	0	0.05	0.12	0.820	99.79
LGR10.2	Chromitite	C2	0.01	0.12	24.45	47.26	0	13.66	0.28	14.02	0.02	0.16	0.01	0.565	99.97
LGR10.3	Chromitite	C2	0.01	0.11	24.84	45.03	3.22	10.87	0.28	16.3	0	0.18	0.1	0.644	100.94
LGR10.7	Chromitite	C2	0	0.1	24.75	45.06	2.76	11.03	0.28	16.07	0	0.19	0.04	0.549	100.28
LGR10.8	Chromitite	C2	0.01	0.11	20.25	50.11	2.58	12.59	0.33	14.77	0	0.09	0	0.550	100.83
LGR10.9s	Chromitite	C2	0.01	0.11	24.39	44.37	3.11	11.94	0.32	15.28	0.01	0.2	0.06	0.624	99.81
LGR13.4c	Chromitite	C2	0.03	0.1	24.57	44.03	3.05	11.96	0.28	15.29	0.01	0.13	0.13	0.550	99.58
LGR06.2	Pyroxenite	C1	0.01	0.16	13.13	52.89	3.07	18.29	0.4	9.55	0	0.11	0.13	0.730	97.72
LGR6.3	Pyroxenite	C1	0.04	0.17	13.41	53.77	2.62	18.82	0.43	9.47	0	0.05	0.3	0.729	99.06
LGR06.21	Pyroxenite	C1	0.06	0.07	14.6	48.99	3.56	24.19	0.58	5.67	0	0.05	0.44	0.692	98.21
LGR06.22	Pyroxenite	C1	0.05	0.06	14.61	48.54	3.66	23.9	0.52	5.74	0.02	0.03	0.45	0.690	97.58

Table 2. Selected analyses (wt. %) of chromite from different rocks of the Logar Ophiolite Complex analysed at the State Geological Institute of Dionýz Štúr in Bratislava, Slovakia. <sup>a</sup> Total FeO

Sample	Location	Lithology	Analytical	Ir	Ru	Pt	Pd	Rh	Au	Total PGE
			Method	ppb	ppb	ppb	ppb	ppb	ppb	
LGR001	C1	Chromitite	M1	-	-	2.6	0.5	12.0	4.0	15.1
LGR002	C1	Dunite	M1	-	-	2.8	3.8	7.0	5.0	13.6
<b>LGR002</b>	<b>C1</b>	<b>Dunite</b>	<b>M2</b>	<b>5.2</b>	<b>17.8</b>	<b>4.4</b>	<b>5.3</b>	<b>0.9</b>	<b>2.1</b>	<b>33.5</b>
LGR003	C1	Chromitite	M1	-	-	2.5	0.8	8.9	4.0	12.2
<b>LGR003</b>	<b>C1</b>	<b>Chromitite</b>	<b>M2</b>	<b>45.1</b>	<b>121.5</b>	<b>7.5</b>	<b>13.8</b>	<b>12.4</b>	<b>3.1</b>	<b>200.2</b>
LGR004	C1	Dunite	M1	-	-	7.4	4.4	3.3	4.0	15.1
LGR006	C1	Pyroxenite	M1	-	-	10.5	2.7	0.3	4.0	13.5
LGR007	C1	Microgabbro	M1	-	-	1.9	<.5	1.6	7.0	3.5
LGR008	C1	Dunite	M1	-	-	5.4	2.4	3.0	7.0	10.8
LGR009	C1	Peridotite	M1	-	-	11.3	16.2	2.8	8.0	30.3
<b>LGR009</b>	<b>C1</b>	<b>Peridotite</b>	<b>M2</b>	<b>4.2</b>	<b>8.3</b>	<b>11.2</b>	<b>18.0</b>	<b>1.6</b>	<b>2.5</b>	<b>43.3</b>
LGR010	C2	Chromitite	M1	-	-	2.1	5.5	16.2	2.0	23.8
LGR011	C2	Chromitite	M1	-	-	5.1	<.5	3.0	2.0	8.1
LGR012	C2	Dunite	M1	-	-	11.3	9.4	1.2	25.0	21.9
<b>LGR012A</b>	<b>C2</b>	<b>Dunite</b>	<b>M2</b>	<b>2.9</b>	<b>6.8</b>	<b>8.1</b>	<b>8.0</b>	<b>1.5</b>	<b>1.7</b>	<b>27.2</b>
<b>LGR012B</b>	<b>C2</b>	<b>Dunite</b>	<b>M2</b>	<b>3.2</b>	<b>7.6</b>	<b>9.7</b>	<b>9.5</b>	<b>1.7</b>	<b>1.5</b>	<b>31.7</b>
LGR013	C2	Chromitite	M1	-	-	6.5	2.1	3.0	12.0	11.6
<b>LGR013</b>	<b>C2</b>	<b>Chromitite</b>	<b>M2</b>	<b>8.7</b>	<b>38.0</b>	<b>9.0</b>	<b>16.6</b>	<b>2.0</b>	<b>4.7</b>	<b>74.2</b>
LGR014	C2	Pyroxenite	M1	-	-	16.1	<.5	1.7	5.0	17.8

Table 3. PGE data for selected samples from localities C1 and C2 in the LOC. M1 = Analysis by lead fire-assay/ICP-MS at ACME labs, Canada. M2 = Analysis by nickel sulphide fire-assay at Cardiff University.



Figure 1. The location of the Logar Ophiolite Complex in Afghanistan.

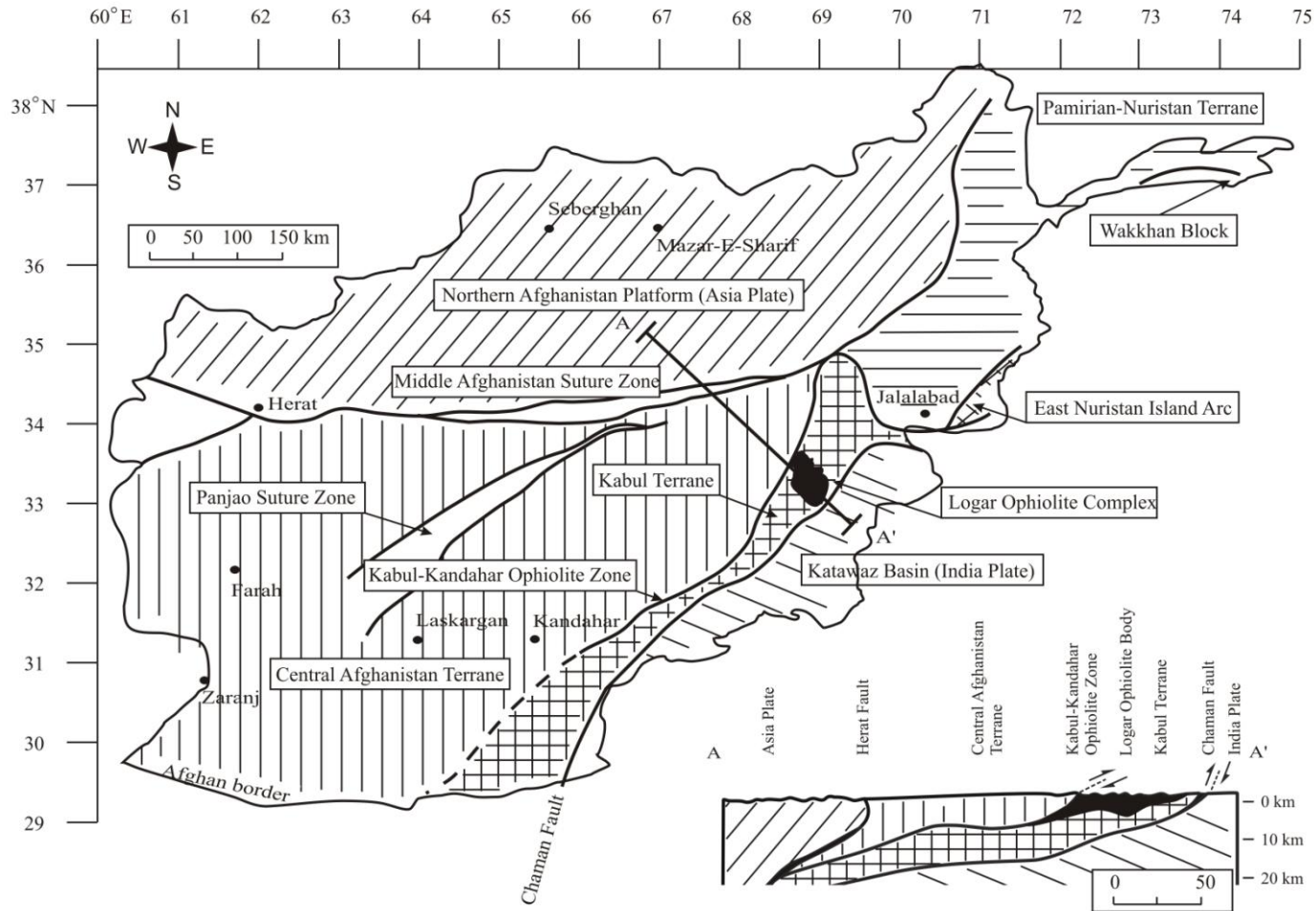


Figure 2. Simplified tectonic map of Afghanistan showing the different terranes in the country.

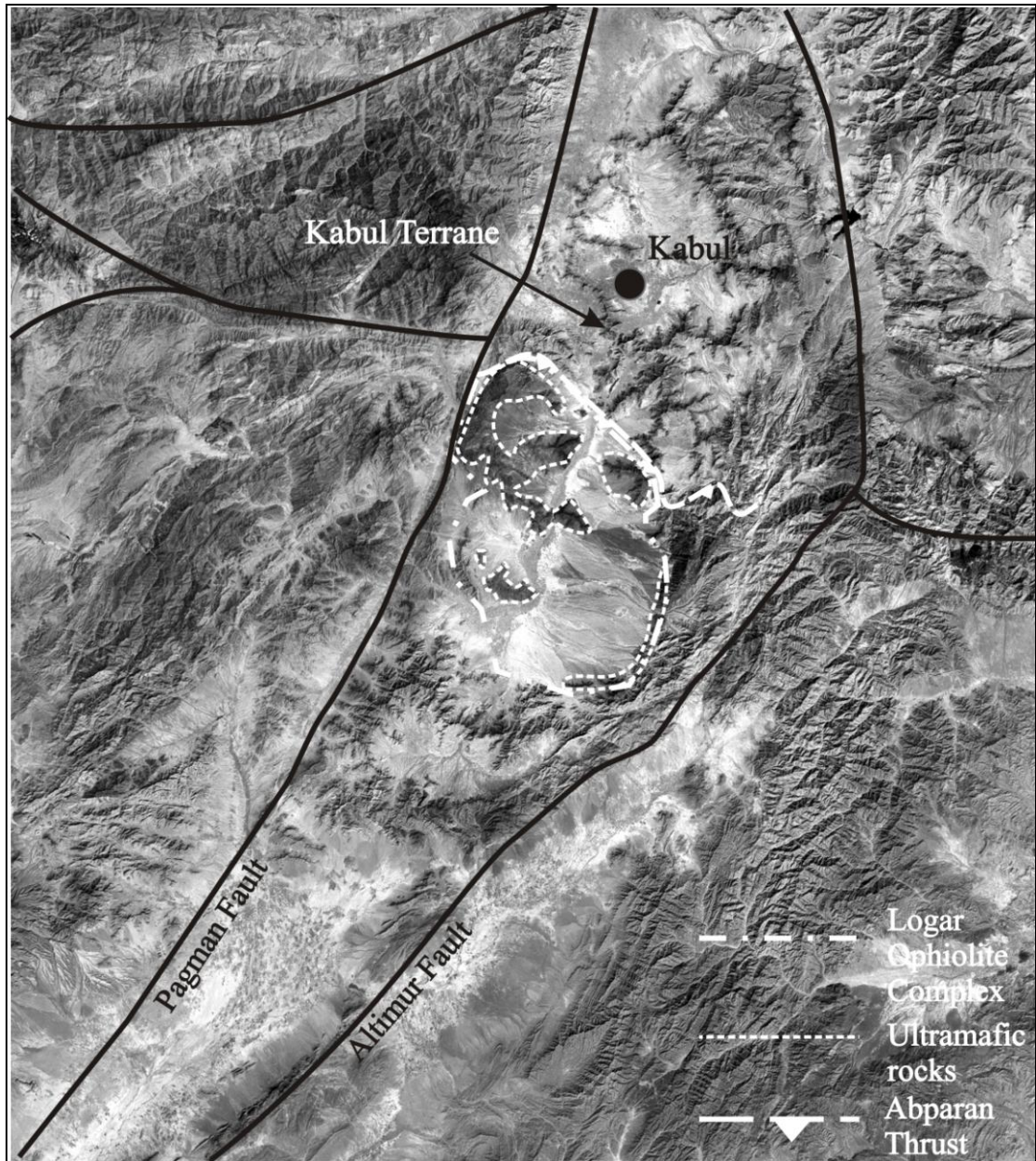


Figure 3. Satellite interpretation of the tectonic setting of the Logar Ophiolite Complex based on Landsat imagery.

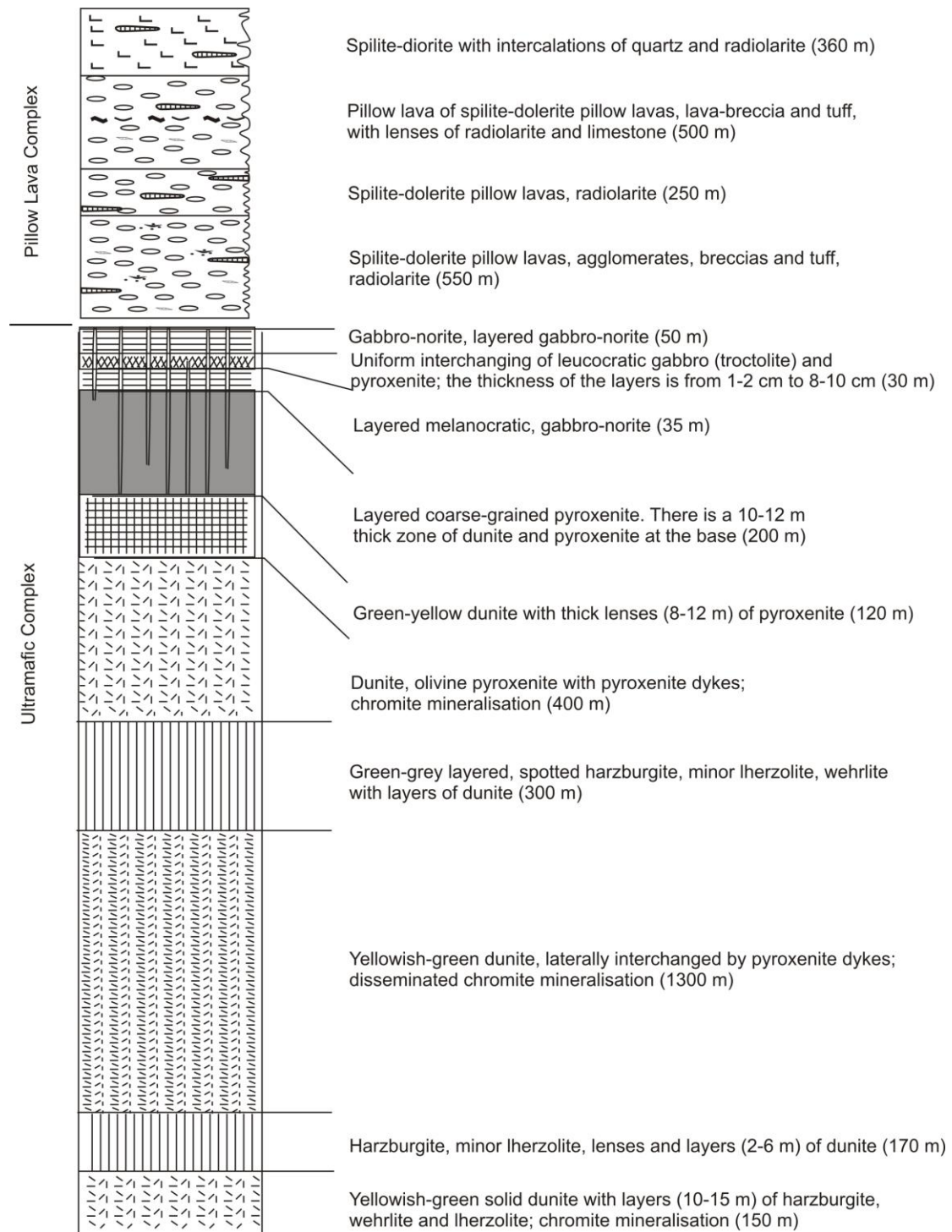


Figure 4. Lithological section through the Ultramafic Complex and Pillow Lava Complex of the Logar Ophiolite Complex. (Modified after Nevretdinov and Mirzamon<sup>30</sup>).

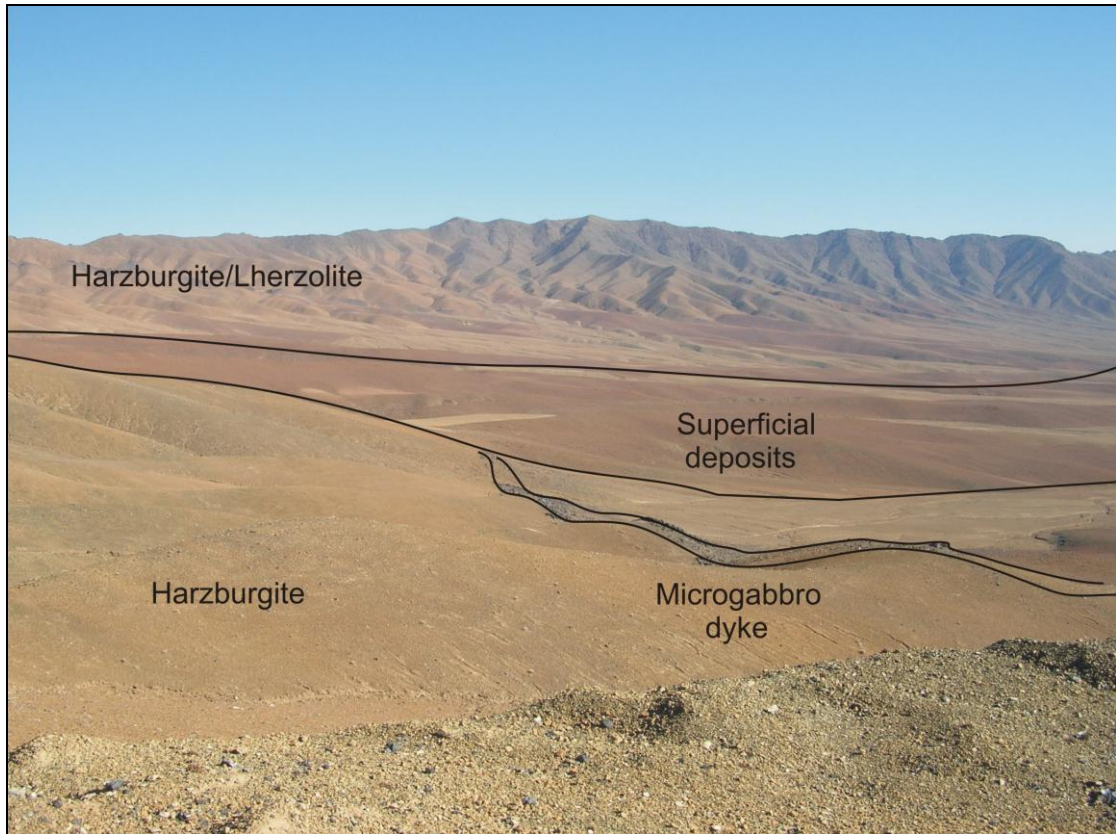


Figure 5. View looking north across the ultramafic part of the LOC. A dyke of microgabbro composition can be seen trending north-west in the mid-background.

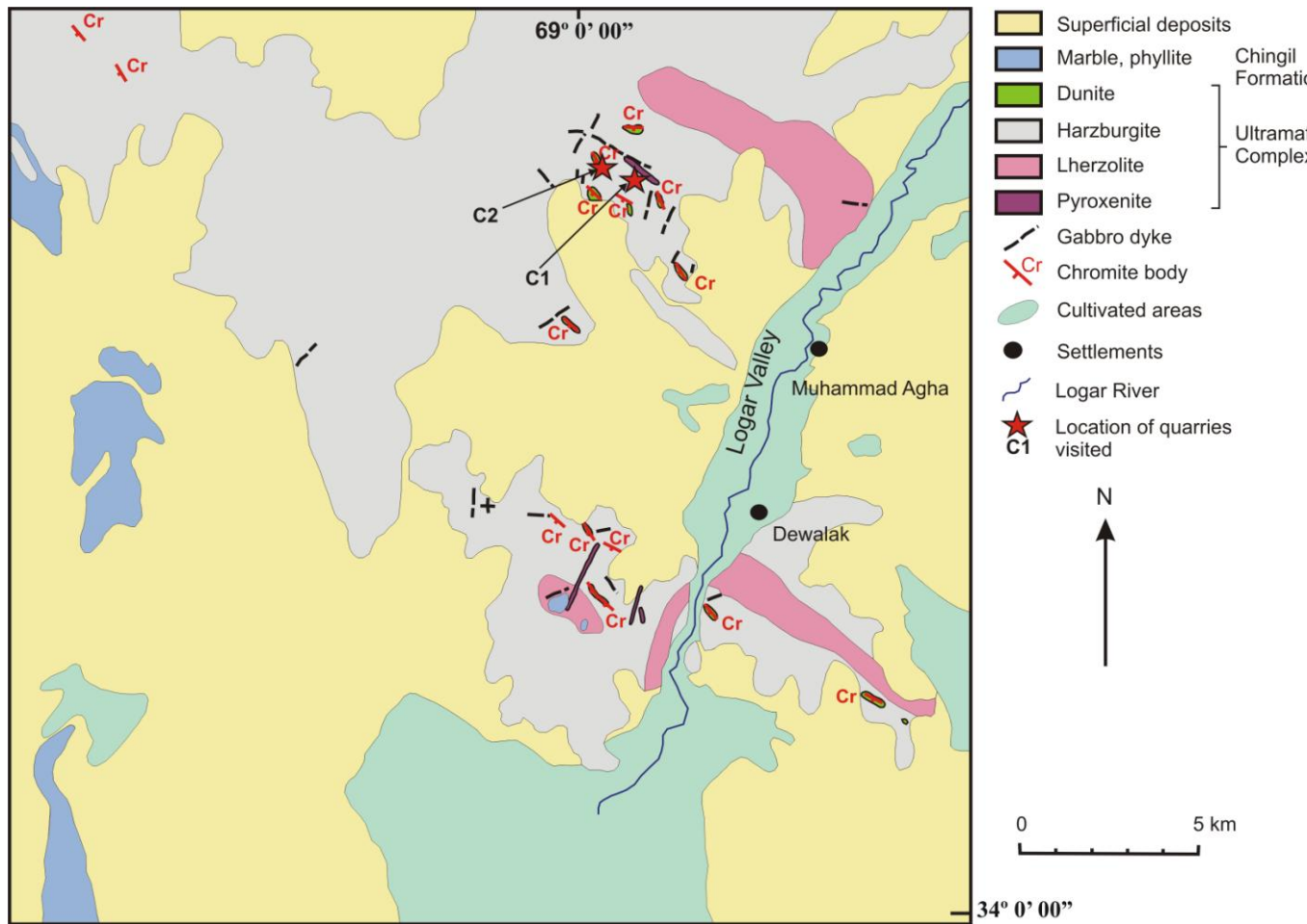


Figure 6. Location of chromite quarries visited, other reported chromite localities and simplified geology of the Logar Ophiolite Complex. Modified from Siebdrat<sup>42</sup>.



Figure 7. First chromite quarry (C1) visited in the Logar Ophiolite Complex ( $34^{\circ} 13' 6.4''$  N,  $69^{\circ} 2' 29.1''$  E) looking west.



Figure 8. Massive chromitite in the side of the C1 chromite quarry ( $34^{\circ} 13' 16.3''$  N,  $69^{\circ} 2' 28.6''$  E)



Figure 9. Disseminated chromite and blebs of chromite associated with carbonate veins in dunite from the C1 chromite quarry (34° 13' 16.3" N, 69° 2' 28.6" E)

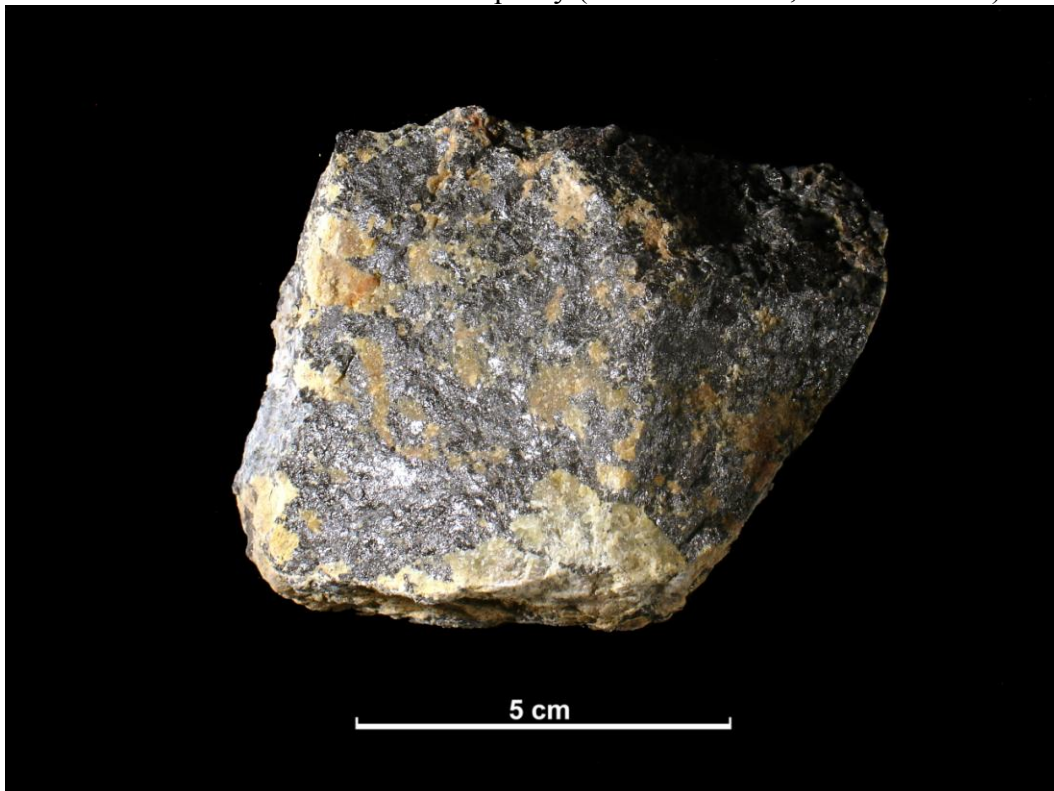


Figure 10. Sub-massive chromite mineralisation taken from the C1 quarry (34° 13' 17.7" N, 69° 2' 28.2" E)



Figure 11. Discordant pyroxenite body (grey) within dunite host (brown) occurring at the western end of the C1 chromite quarry (34° 13' 17.7" N, 69° 2' 28.2" E)

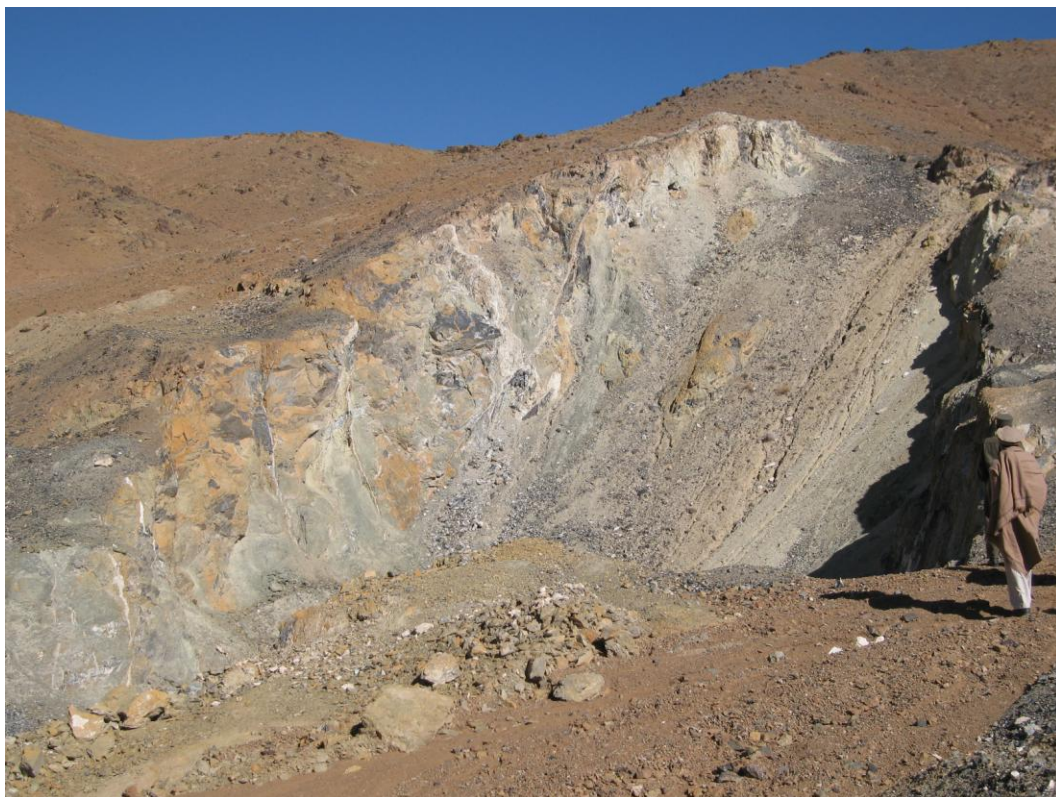


Figure 12. Second quarry (C2) visited in the Logar Ophiolite Complex (34° 13' 43.6" N, 69° 1' 34.3" E). Lithologies exposed in the quarry wall include pyroxenite (grey), dunite (brown), and carbonitised ultramafic rocks (white)

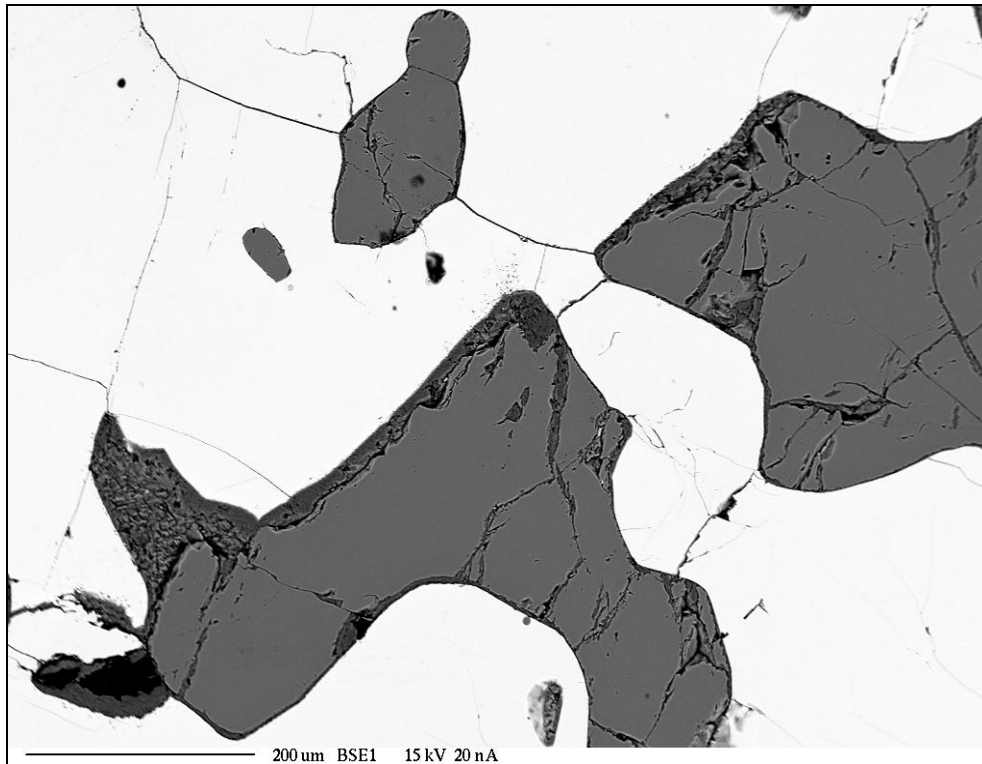


Figure 13. SEM photomicrograph of LGR 010 (chromitite) from C1 showing interlocking chromite crystals (white) and interstitial olivine (light grey) being replaced by serpentine (lizardite) (dark-grey)

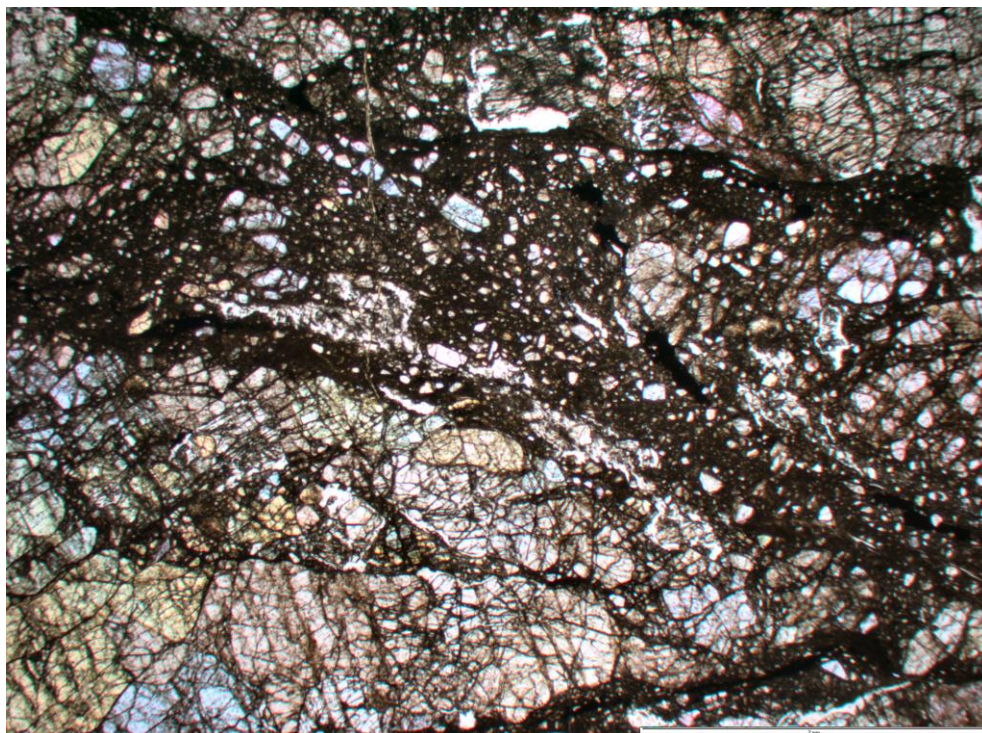


Figure 14. Photomicrograph of dunite (LGR 012) in plane polarised light. Note cataclasite zone of crushed olivine through the sample. Scale bar 2 mm.

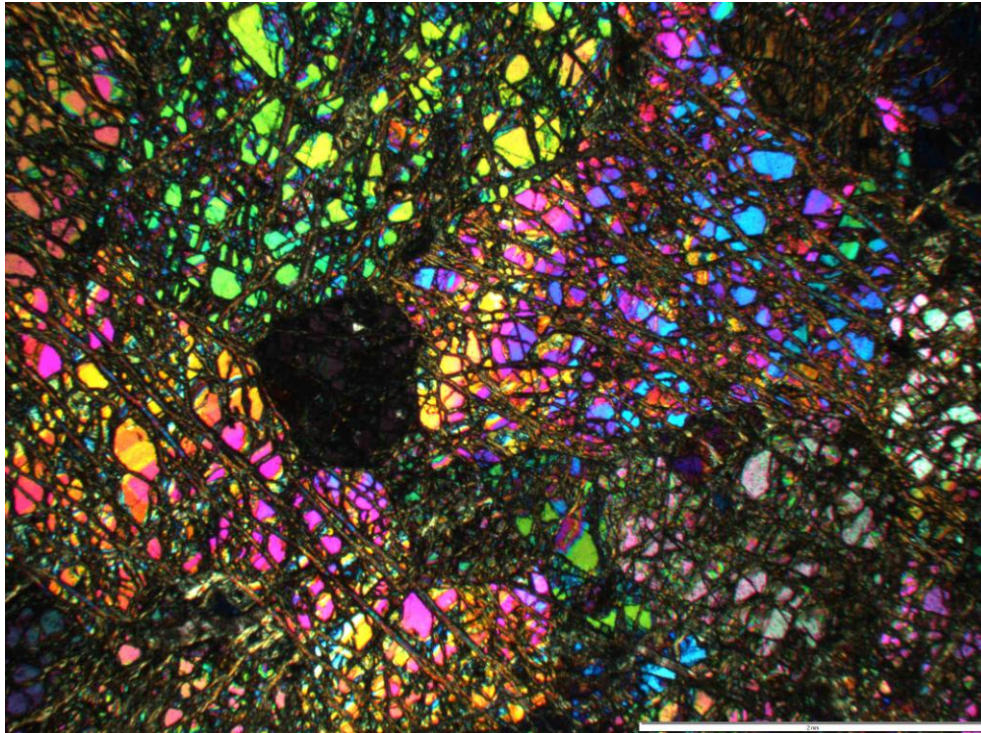


Figure 15. Photomicrograph of peridotite (LGR 009) in cross polarised light. The olivine (highly coloured) is very fresh and comparatively unaltered. Note the opaque chromite inclusions (black). Scale bar 2 mm.



Figure 16. Photomicrograph of LGR 005 (pyroxenite - websterite) in cross polarised light showing typically fresh, unaltered diopside crystals. Scale bar 2 mm.

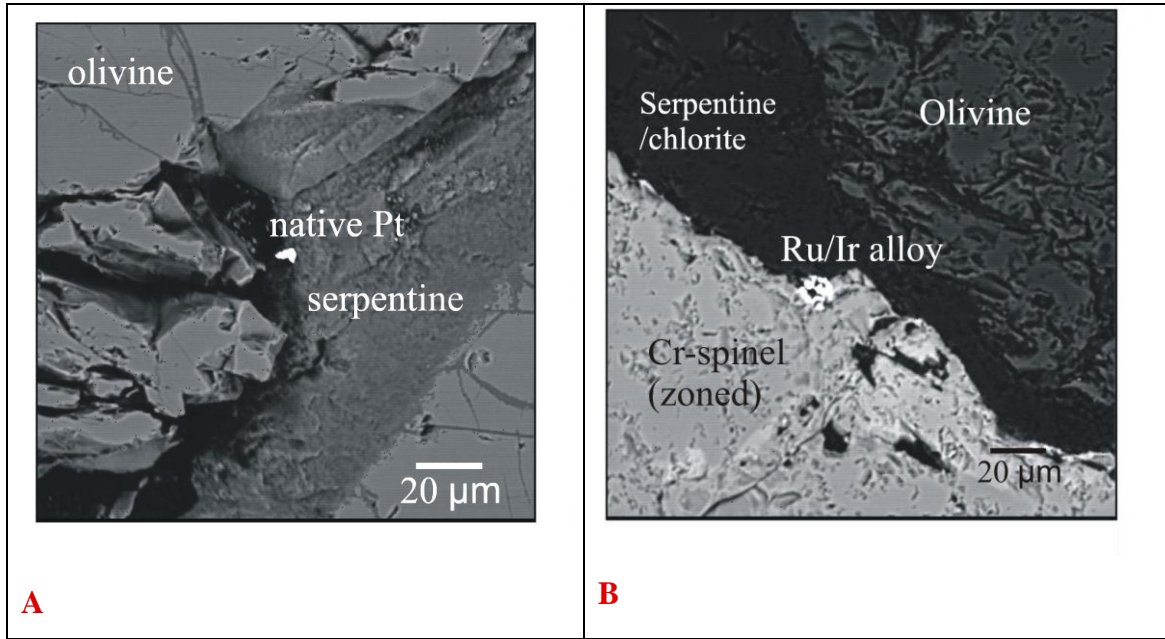


Figure 17 A) Sample LGR 012 (dunite), a grain of native Pt (+Fe) found associated with serpentinised olivine, and, B) Sample LGR 013 (chromitite), a grain of Ru-Ir alloy found along an altered olivine/Cr-spinel boundary.

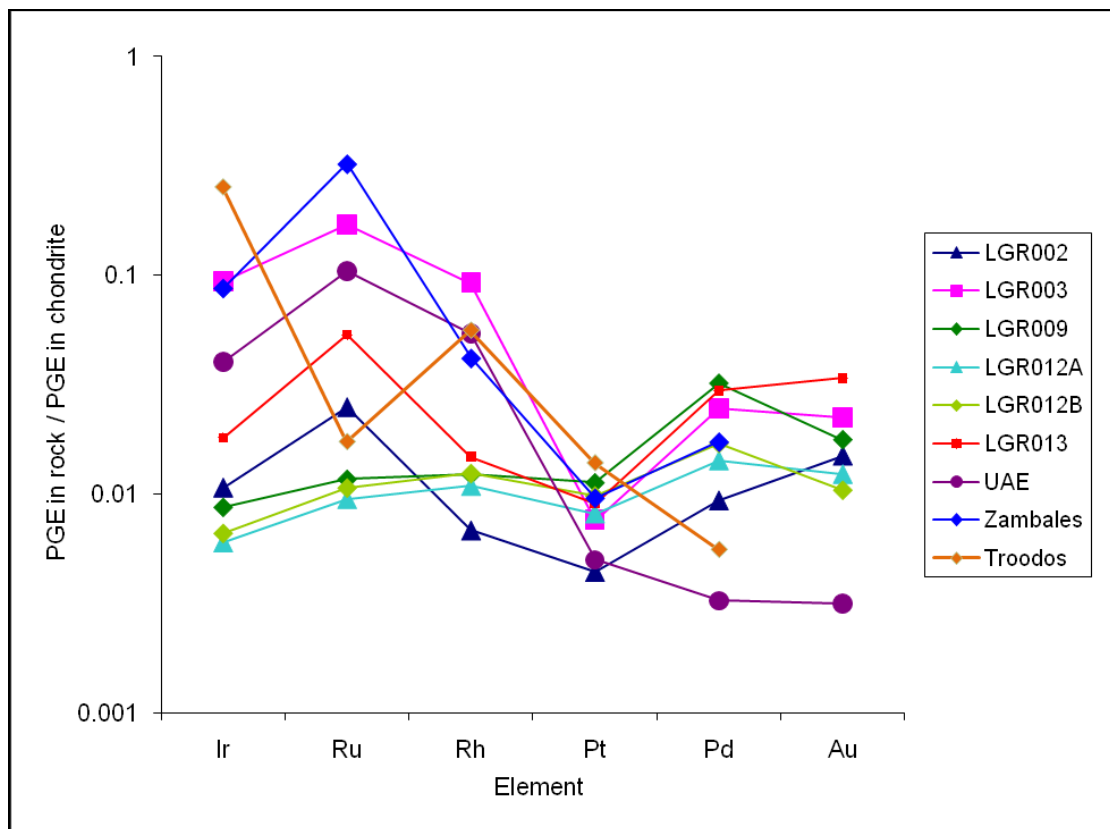


Figure 18. Chondrite-normalised plots of samples from C1 and C2. Chondrite PGE levels from Anders and Grevesse<sup>4</sup>. UAE data taken from Dare (pers. comm.), Zambales data from Bacuta et al<sup>9</sup> Troodos data from Prichard and Lord<sup>36</sup>.

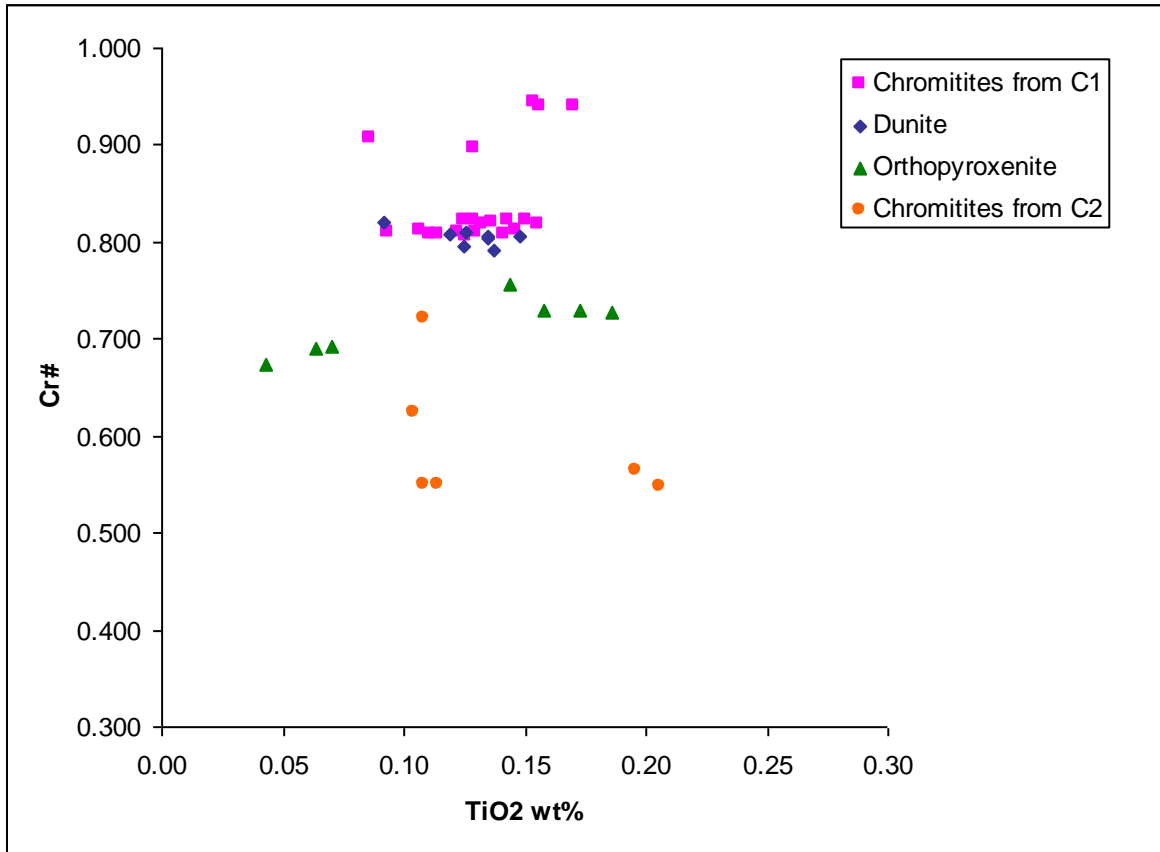


Figure 19. Cr# (Cr/(Cr + Al)) v TiO<sub>2</sub> for the chromite samples from the LOC.

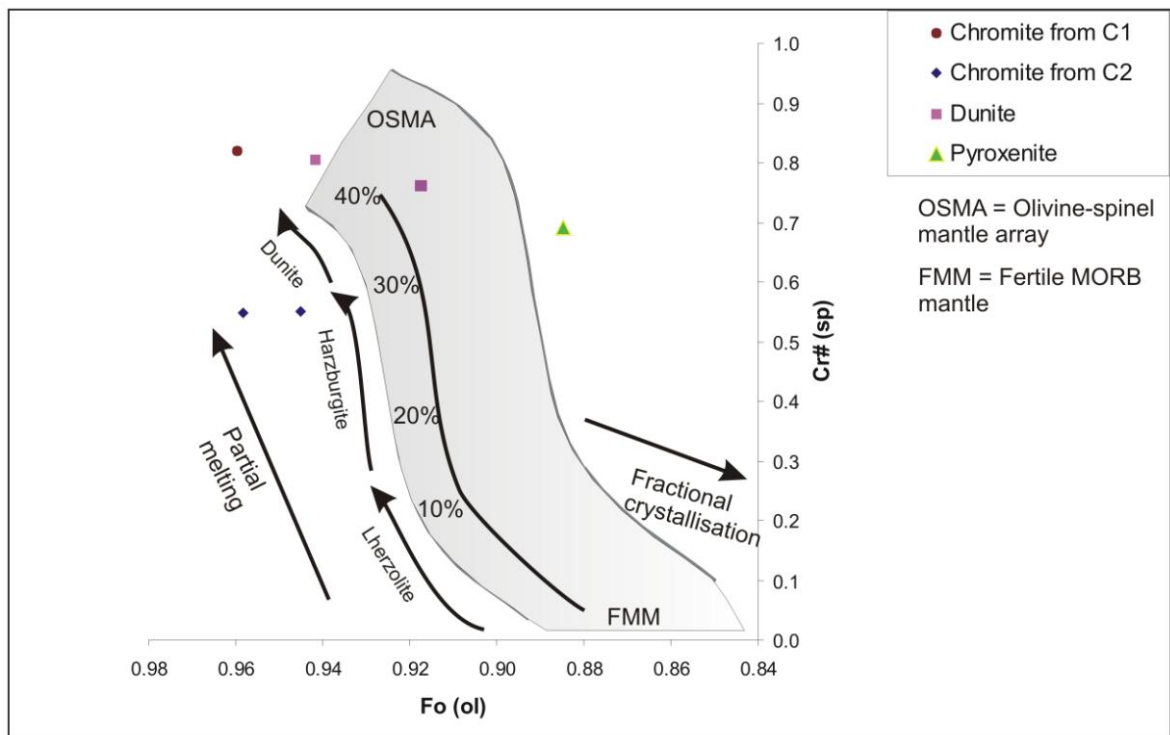


Figure 20. Cr# spinel against olivine Fo content for rock samples taken from C1 and C2. The diagram shows the olivine-spinel mantle array (OSMA) and melting trend (annotated by % melting) of Arai<sup>6</sup> and the fractional crystallization trend to lower Fo<sup>7</sup>.

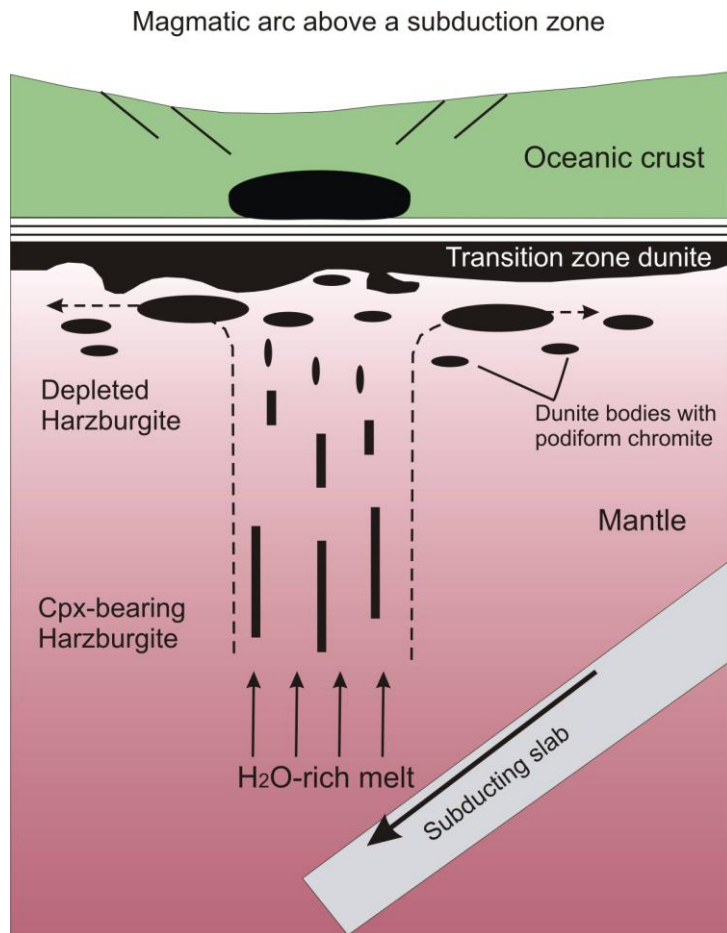


Figure 21. Model for the formation of podiform chromite deposits in a supra-subduction zone.